



# EUROPEAN SOUTHERN OBSERVATORY

Organisation Européenne pour des Recherches Astronomiques dans l'Hémisphère Austral  
Europäische Organisation für astronomische Forschung in der südlichen Hemisphäre

ESO - European Southern Observatory  
Karl-Schwarzschild Str. 2, D-85748 Garching bei München

---

## Very Large Telescope

# HAWK-I User Manual

Doc. No. VLT-MAN-ESO-14800-3486

Issue 113  
Feb 2024

Prepared ..... M. Berton and the HAWK-I IOT .....

Approved ..... S. Mieske .....

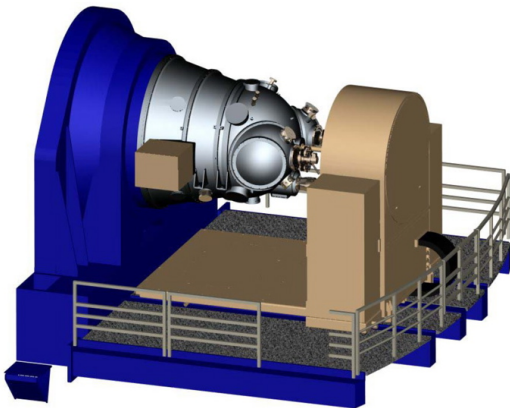
| Name | Date | Signature |
|------|------|-----------|
|------|------|-----------|

Released ..... A. Kaufer .....

| Name | Date | Signature |
|------|------|-----------|
|------|------|-----------|

### Change Record

| Issue/Rev.  | Date         | Section/Parag. affected | Reason/Initiation/Documents/Remarks  |
|-------------|--------------|-------------------------|--|
| Issue 93.0  | 06 Jan 2014  |                         | Fast Photometry update   |
| Issue 94.0  | 28 Jan 2014  |                         | USD comments implemented   |
| Issue 94.1  | 07 Jun 2014  |                         | Corrected several typos. Added a figure.   |
| Issue 95    | 27 Aug 2014  |                         | No news.   |
| Issue 96    | 22 Jan 2015  |                         | Add a description of Adapter defocusing.   |
| Issue 96    | 10 Jun 2015  |                         | Add reference to the GUCT, to the ETC seeing/IQ, USD comments implemented, fix broken links  |
| Issue 99    | 22 Jan 2017  |                         | No news.   |
| Issue 100   | 07 May 2017  |                         | Changes to the pipeline section.   |
| Issue 102   | March 2018   |                         | New section to describe GRAAL. General organization reviewed.  |
| Issue 103.0 | August 2018  |                         | Many different small changes. Additional information for GRAAL+HAWK-I.   |
| Issue 104   | Dec. 2018    |                         | Elimination of the Burst mode section.   |
| Issue 105   | Aug. 2019    |                         | Add turbulence constraints information.  |
| Issue 106   | 18 Feb. 2020 |                         | Add the transformations from the 2MASS magnitudes to the magnitudes in the HAWK-I filters  |
| Issue 106.1 | 22 May 2020  |                         | Highlight the TTS is not available currently.  |
| Issue 107   | 23 Nov 2020  |                         | replace the GuideCam tools with ObsPrep, add p2fc for finding chart generation, and add ESO Phase 2 API                            |
| Issue 108   | 11 Feb 2021  |                         | add more details on SATLEVEL for Non-Destructive Read and DoubleRdRstRD modes  |
| Issue 108.1 | 1 June 2021  |                         | update the new user support system and filter replacement procedure  |
| Issue 111   | 1 Sep 2022   |                         | update the detector GAIN value and format of the transformations from the 2MASS magnitudes to the magnitudes in the HAWK-I filters |
| Issue 113   | 12 Feb 2024  |                         | update on the usage of NB filters  |



HAWK-I as a CAD drawing attached to the VLT and in the integration hall in Garching

### HAWK-I in a Nutshell

Online information on HAWK-I can be found on the [instrument web pages](#), in [Casali et al. 2006](#), and in [Kissler-Patig et al. 2008](#).

HAWK-I is a near-infrared ( $0.9 - 2.5 \mu\text{m}$ ) wide-field imager.

The instrument is cryogenic (120 K, detectors at 75 K) and has a full reflective design. The light passes four mirrors and two filter wheels before hitting a mosaic of four Hawaii 2RG  $2048 \times 2048$  pixels detectors. The final F-ratio is F/4.36 ( $1''$  on the sky correspond to  $169.4 \mu\text{m}$ ).

The field of view (FoV) on the sky is  $7.5' \times 7.5'$  (with a small cross-shaped gap of  $\sim 15''$  between the four detectors). The pixel scale is  $0.106'' / \text{pix}$ . The two filter wheels of six positions each host ten filters: Y, J, H,  $K_s$  (identical to the [VISTA](#) filters), as well as 6 narrow band filters ( $\text{Br}\gamma$ ,  $\text{CH}_4$ ,  $\text{H}_2$  and four cosmological filters at 0.984, 1.061, 1.187, and  $2.090 \mu\text{m}$ ).

Typical limiting magnitudes ( $S/N=5$  in 3600s on source) are around  $J= 23.9$ ,  $H= 22.5$  and  $K_s= 22.3$  mag (Vega).

HAWK-I can be used in combination with the GROUND layer Adaptive optics system Assisted by Lasers (GRAAL), a seeing improver, whose ultimate goal is to enhance the instrument image quality. Under most seeing conditions ( $1''$  in visible band), with the use of 4 lasers and telescope correction GRAAL reduces the 50% encircled energy diameter by 12% in the Y and 21% in the  $K_s$  filters, respectively, over the entire FoV. That is, the FWHM of the PSF is typically reduced from  $0.53''$  to  $0.42''$  in  $K_s$  band.

Observations with GRAAL require PHO, CLR or THN conditions.

# Contents

|           |   |           |
|-----------|---|-----------|
| <b>1</b>  | <b>Introduction</b>                                       | <b>1</b>  |
| 1.1       | Science drivers . . . . .                                 | 1         |
| 1.2       | Scope of this document . . . . .                          | 1         |
| 1.3       | Structure of this document . . . . .                      | 1         |
| 1.4       | More important information . . . . .                      | 2         |
| 1.5       | Contact information . . . . .                             | 2         |
| 1.6       | News . . . . .  | 2         |
| 1.7       | Glossary . . . . .  | 2         |
| 1.8       | Abbreviations and Acronyms . . . . .                      | 3         |
| <br>      |   |           |
| <b>I</b>  | <b>The instrument</b>                                     | <b>4</b>  |
| <br>      |   |           |
| <b>2</b>  | <b>Cold part: the imager</b>                              | <b>4</b>  |
| 2.1       | Optics . . . . .  | 4         |
| 2.2       | Mechanics . . . . .                                       | 5         |
| 2.3       | Detectors . . . . .                                       | 5         |
| <br>      |   |           |
| <b>3</b>  | <b>Warm part: the ground layer adaptive optics system</b> | <b>5</b>  |
| 3.1       | Introduction . . . . .                                    | 6         |
| 3.1.1     | Atmospheric Turbulence . . . . .                          | 6         |
| 3.1.2     | Ground Layer Adaptive Optics . . . . .                    | 6         |
| 3.2       | Design of the module . . . . .                            | 7         |
| 3.3       | Wavefront sensors . . . . .                               | 8         |
| <br>      |   |           |
| <b>II</b> | <b>Instrument Performance</b>                             | <b>9</b>  |
| <br>      |   |           |
| <b>4</b>  | <b>Detectors</b>  | <b>9</b>  |
| 4.1       | Threshold-limited integration . . . . .                   | 10        |
| <br>      |   |           |
| <b>5</b>  | <b>Field of view</b>                                      | <b>10</b> |
| 5.1       | Relative position of the four quadrants . . . . .         | 12        |
| 5.2       | Center of Rotation and Centre of Pointing . . . . .       | 12        |
| 5.3       | Vignetting of the FoV . . . . .                           | 13        |
| <br>      |   |           |
| <b>6</b>  | <b>Filters</b>  | <b>13</b> |
| <br>      |   |           |
| <b>7</b>  | <b>Limiting magnitudes</b>                                | <b>14</b> |
| <br>      |   |           |
| <b>8</b>  | <b>Image quality and astrometry</b>                       | <b>15</b> |



|  |           |
|--|-----------|
| <b>III Observing with HAWK-I: from phase 1 to data reduction</b> | <b>17</b> |
| <b>9 Introduction</b>  | <b>17</b> |
| <b>10 Phase 1: applying for observing time with HAWK-I</b>       | <b>17</b> |
| 10.1 Getting reasonable photometry with HAWK-I . . . . .         | 18        |
| 10.1.1 Consider the 2MASS calibration fields . . . . .           | 18        |
| 10.1.2 HAWK-I extinction coefficients . . . . .                  | 18        |
| 10.2 The Exposure Time Calculator . . . . .                      | 19        |
| 10.3 Proposal Form . . . . .                                     | 19        |
| 10.4 Overheads and Calibration Plan . . . . .                    | 20        |
| <b>11 Phase 2: preparing your HAWK-I observations</b>            | <b>22</b> |
| 11.1 HAWK-I specifics to templates, OBs, and p2 . . . . .        | 22        |
| 11.1.1 HAWKI p2 . . . . .  | 22        |
| 11.1.2 Observing Blocks – OBs . . . . .                          | 22        |
| 11.1.3 Templates . . . . .                                       | 22        |
| 11.1.4 Finding Charts and README Files . . . . .                 | 23        |
| 11.1.5 ObsPrep tools . . . . .                                   | 24        |
| 11.1.6 ESO Phase 2 API . . . . .                                 | 24        |
| <b>12 Observing strategies with HAWK-I</b>                       | <b>25</b> |
| 12.1 Overview . . . . .  | 25        |
| 12.2 Visitor Mode Operations . . . . .                           | 25        |
| 12.3 The influence of the Moon . . . . .                         | 25        |
| 12.4 Twilight . . . . .  | 25        |
| 12.5 Orientation, offset conventions and definitions . . . . .   | 26        |
| 12.6 Instrument and telescope overheads . . . . .                | 27        |
| 12.7 Recommended DIT/NDIT and Object–Sky pattern . . . . .       | 27        |
| <b>IV Reference Material</b>                                     | <b>30</b> |
| <b>A The HAWK-I detectors</b>                                    | <b>30</b> |
| A.1 Threshold-limited integration . . . . .                      | 31        |
| A.2 Detectors’ structures and features . . . . .                 | 31        |
| A.3 Detectors’ relative sensitivity . . . . .                    | 33        |
| <b>B The HAWK-I filters</b>                                      | <b>34</b> |
| <b>C The HAWK-I calibration plan</b>                             | <b>35</b> |
| C.1 Do you need special calibrations? . . . . .                  | 35        |
| C.2 The HAWK-I standard calibrations in a nutshell . . . . .     | 36        |

|          |  |           |
|----------|--|-----------|
| C.3      | Quality Control . . . . .  | 38        |
| <b>D</b> | <b>HAWK-I Fast Jitter Mode</b>   | <b>39</b> |
| D.1      | Description . . . . .  | 39        |
| D.2      | Implementation . . . . .   | 40        |
| D.2.1    | Detector Windowing . . . . .   | 40        |
| D.2.2    | Data Products and Cube Sizes . . . . .   | 41        |
| D.2.3    | Minimum DIT, Overheads, and Frame Losses . . . . .                               | 43        |
| D.3      | Preparation and Observation . . . . .  | 45        |
| D.3.1    | OB Naming Convention . . . . .   | 45        |
| D.3.2    | OB Requirements and Finding Charts . . . . .                                     | 45        |
| D.3.3    | Observing Modes . . . . .  | 45        |
| D.3.4    | Calibration Plan . . . . .   | 45        |
| D.3.5    | FITS Files Names . . . . .   | 47        |
| D.4      | Template Guide . . . . .   | 47        |
| D.4.1    | Acquisition: <i>HAWKI_img_acq_FastPhot</i> and <i>HAWKI_img_acq_LGS_FastPhot</i> | 47        |
| D.4.2    | Science template: <i>HAWKI_img_obs_FastPhot</i> . . . . .                        | 47        |
| D.4.3    | Calibration templates: <i>HAWKI_img_cal_DarksFastPhot</i> . . . . .              | 48        |

# 1 Introduction

HAWK-I does only one thing, but it does it well: direct imaging in the NIR (0.9 to 2.5  $\mu\text{m}$ ) over a large field (7.5'  $\times$  7.5'). It can be used in seeing limited mode, but also it can make use of ground layer adaptive optics (GRAAL) achieved through a deformable secondary mirror and the laser guide stars facility.

## 1.1 Science drivers

So far HAWK-I has been successfully used to study:

- the properties of medium redshift galaxy clusters (see e.g. Lidman et al. 2008, A&A 489,981)
- the outer solar system bodies (see e.g. Snodgrass et al. 2010, A&A 511, 72),
- the very high redshift universe (see e.g. Castellano et al. 2010, A&A 511, 20),
- exo-planets (see e.g. Gillon et al. 2009, A&A 506, 359),
- the properties of Galactic stellar populations (see e.g. Valenti et al. 2013, A&A, 559, 98) and star-forming regions (see e.g. Preibish et al. 2011, A&A, 530, 34)

The implementation of Fast Photometry (see Appendix F) allows high time resolution observations, such as to follow the lightcurve of x-ray binaries, as well as to study crowded fields through holographic imaging techniques (see Schoedel et al. 2013, MNRAS, 249, 1367)

## 1.2 Scope of this document

The HAWK-I user manual provides a description of the instrument characteristics, as well as information required for the proposal (Phase 1) and the observation (Phase 2) preparation. Guidelines for the post-observation phase are also summarised.

The instrument has started regular operations in period 81 operating exclusively in seeing limited mode until period P101. Afterwards, with the installation of the Adaptive Optics Facility (AOF) on UT4 the instrument has been equipped with GRAAL, a seeing improver allowing to enhance the instrument image quality. The system GRAAL + HAWK-I is offered since P102.

We welcome any comments and suggestions on the present manual; these should be addressed to ESO User Support Department via <https://support.eso.org>.

## 1.3 Structure of this document

The document is structured as follows:

- Part I provides a technical description of HAWK-I and GRAAL;
- Part II details the instrument performance;
- Part III describes the commonly used observing technique in the IR and provides guidelines for Phase 1 and Phase 2 preparation;
- Part IV contains collected useful reference material.

## 1.4 More important information

One thing you must remember is:

- Phase 1 constraints are binding.

All HAWK-I related manuals are available on the [HAWK-I instrument web page](#) together with the most updated information of the instrument.

For both Service and Visitor mode Observing Block (OBs) should be prepared with the web-based Phase 2 Proposal Preparation (p2) ([p2](#)).

Information on the preparation of Service mode observation with HAWK-I can be found [here](#).

Visiting astronomers do not need to submit OBs in advance of their observations. However, they should prepare them before arriving at the observatory or, at latest, at the observatory the nights before their observing run. They will find further instructions on the [Paranal Science Operations web page](#) and the [Paranal Observatory home page](#). In particular, visiting astronomers are strongly encouraged to read this [page](#).

## 1.5 Contact information

In case of specific questions related to Service Mode observations, the use of the pipeline, and the proposal preparation (Phase 1) please contact the ESO User Support Department via <https://support.eso.org>.

For general information on Visitor Mode observations please contact the [Paranal Science Operation Team](#).

## 1.6 News

Please recall that the most up-to-date information on the instrument can be found on the [HAWK-I news web page](#).

## 1.7 Glossary

**Active Optics:** This is the active control of the primary mirror of the telescope. It is performed by using a telescope guide star.

**Adaptive Optics:** This is the correction of the wavefront errors induced by atmospheric turbulence. The wavefront is measured from laser spots and the corresponding corrections are sent to the deformable secondary mirror.

**Laser Guide Star:** The artificial star created by the sodium laser at an altitude of ~80-100 km.

**Tip-Tilt Star:** The star used to sense and correct the tip-tilt aberrations, which are not sensed by the lasers. **At current stage, HAWK-I AO observations is in Tip-Tilt Star (TTS) free mode. Therefore, TTS is not required.**

## 1.8 Abbreviations and Acronyms

|               |  |
|---------------|--|
| <b>2MASS</b>  | Two Micron All Sky Survey                              |
| <b>4LGS</b>   | 4 Laser Guide Stars                                    |
| <b>AO</b>     | Adaptive Optics  |
| <b>AOF</b>    | Adaptive Optics Facility                               |
| <b>DIT</b>    | Detector Integration Time                              |
| <b>DMO</b>    | Data Management and Operations Division                |
| <b>DSM</b>    | Deformable Secondary Mirror                            |
| <b>ESO</b>    | European Southern Observatory                          |
| <b>ETC</b>    | Exposure Time Calculator                               |
| <b>FC</b>     | Finding Chart  |
| <b>FoV</b>    | Field of View  |
| <b>FWHM</b>   | Full Width at Half Maximum                             |
| <b>GLAO</b>   | Ground Layer Adaptive Optics                           |
| <b>GRAAL</b>  | GRound layer Adaptive optics system Assisted by Lasers |
| <b>HAWK-I</b> | High Acuity Wide-field K-band Imager                   |
| <b>NDIT</b>   | Number of Detector Integration Time                    |
| <b>NGS</b>    | Natural Guide Star                                     |
| <b>NIR</b>    | Near InfraRed  |
| <b>OB</b>     | Observing Block  |
| <b>P2PP</b>   | Phase II Proposal Preparation                          |
| <b>PSF</b>    | Point Spread Function                                  |
| <b>QC</b>     | Quality Control  |
| <b>RTC</b>    | Real Time Computer                                     |
| <b>RTD</b>    | Real Time Display                                      |
| <b>SM</b>     | Service Mode   |
| <b>TT</b>     | Tip-Tilt   |
| <b>TIO</b>    | Telescope and Instrument Operator                      |
| <b>USD</b>    | User Support Department                                |
| <b>UT</b>     | Unit Telescope   |
| <b>VLT</b>    | Very Large Telescope                                   |
| <b>VM</b>     | Visitor Mode   |
| <b>WF</b>     | WaveFront  |
| <b>WFS</b>    | WaveFront Sensor                                       |

## Part I

# The instrument

## 2 Cold part: the imager

The HAWK-I instrument design is presented by Casali et al. 2006, and Kissler-Patig et al. 2008; a summary is provided in the following subsections.

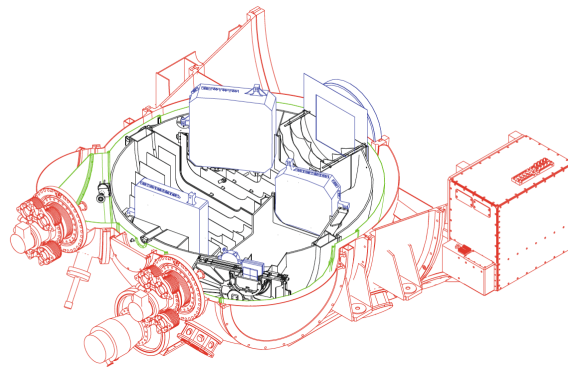


Figure 1: Cut through HAWK-I for an optical and mechanical overview. Blue: optical components; black: cold assembly, filter wheels, detector assembly; green: radiation shield; red: vessel structure, cryogenic components, electronic rack.

### 2.1 Optics

The optical layout of HAWK-I is given in Fig. 2. The entrance window of the vacuum vessel is

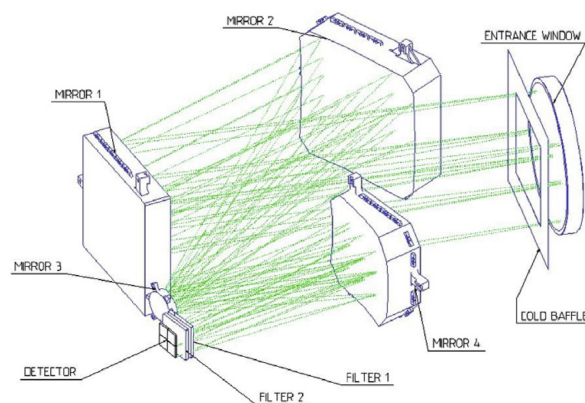


Figure 2: HAWK-I optical layout

used to image the pupil on the M3 mirror. A cold baffle stops the light outside of the instrument FoV. The first folding mirror (M1) is used for beam accommodation. Then the camera consists of one large spherical mirror M2 and two aspherical mirrors M3 and M4 allowing to adapt the

telescope beam to the required  $F/4.36$ . The two filter wheels are located directly in front of the detector mosaic. The size of the filter needed to cover the whole FoV is  $105 \times 105$  mm. The beam incidence angle versus the filter is quasi constant for all points of the field to keep the spectral filtering uniform over the whole FoV.

## 2.2 Mechanics

HAWK-I is installed at the Nasmyth A of VLT-UT4 (Yepun), and centred on the Nasmyth adaptor by the interface flange. The vacuum vessel is split into three elements: *i*) vessel front part, which extends to the interface flange diameter; *ii*) vessel centre part, which offers all necessary supply ports and mechanical connections to support the cold mechanics; *iii*) access to the detector, filter unit, filter exchange, the connection of the closed cycle coolers, pre-cooling lines and electronically cables.

## 2.3 Detectors

The HAWK-I detector mosaic (see Fig. 3) is composed of four  $2k \times 2k$  Hawaii 2RG arrays with  $2.5 \mu\text{m}$  cutoff.

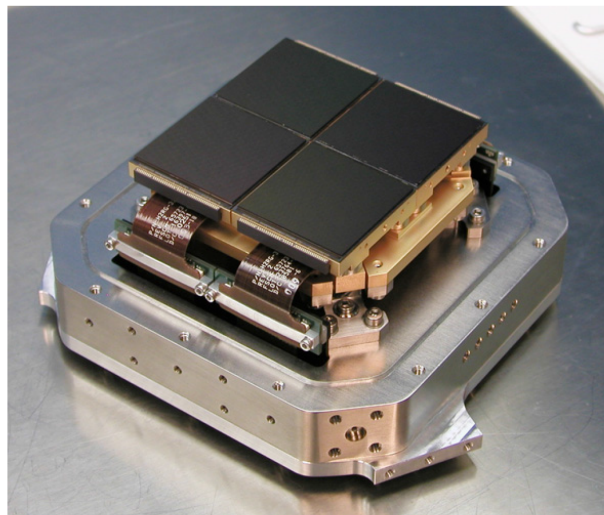


Figure 3: HAWK-I detector mount

## 3 Warm part: the ground layer adaptive optics system

GRAAL, the ground layer adaptive optics system of HAWK-I is presented and discussed in [Paufigue et al 2010](#) and [Paufigue et al. 2012](#).

The adaptive correction (AO) is provided by the deformable secondary mirror (DSM), nearly conjugated with the ground layers of the atmosphere, at  $\sim 90$  m. Therefore GRAAL is able to compensate for the lowest layers of the atmospheric turbulence (up to  $\sim 1$  km, depending on the spatial frequencies considered), carrying more than half of the turbulence variance. GRAAL is a seeing improver, and does not provide diffraction limited images at the focal plane. To highlight the advantage of

combining GRAAL with HAWK-I a PSF is shown in Fig. 4 in AO open-loop (uncorrected) and a close-loop.

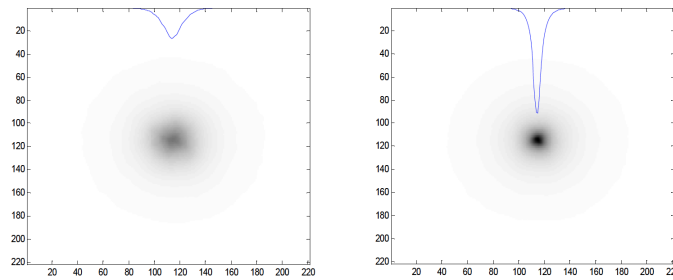


Figure 4: Observed PSF without (*left*) and with (*right*) GRAAL correction.

## 3.1 Introduction

The following section provides an introduction to the field of atmospheric turbulence, and it is essentially taken from the NACO user manual. For further reading, see for example *Adaptive Optics in astronomy*, Rodier 1999, Cambridge University Press, or *Introduction to adaptive optics*, Tyson 2000, Bellinghan/SPIE.

### 3.1.1 Atmospheric Turbulence

The VLT theoretical diffraction limit is  $1.22 \times \lambda/D = 0.07''$  at  $\lambda = 2.2 \mu\text{m}$ . However, the resolution is severely limited by the atmospheric turbulence to  $\lambda/r_0 \sim 1''$ , where  $r_0$  is the Fried parameter.  $r_0$  is directly linked to the strength of the turbulence and it depends on the wavelength as  $\lambda^{6/5}$ . For average observing conditions,  $r_0$  is typically 60 cm at  $2.2 \mu\text{m}$ .

Temperature inhomogeneities in the atmospheric induce temporal and spatial fluctuations in the air refractive index and therefore cause fluctuations in the optical path. This leads to random phase delay that corrugate the wavefront. The path differences are, to a good approximation, achromatic. Only the phase of the wavefront (WF) is chromatic. The coherence time of the WF distortions is related to the average wind speed  $V$  in the atmosphere and is typically of the order of  $r_0/V = 60 \text{ ms}$  at  $2.2 \mu\text{m}$  for  $V = 10 \text{ m/s}$ .

### 3.1.2 Ground Layer Adaptive Optics

A technique to overcome the degrading effects of the atmospheric turbulence is real-time compensation of the deformation of the WF by AO. Very schematically, the wavefront sensor (WFS) measures the WF distortions, which are processed by the real-time computer (RTC). The RTC controls a deformable mirror to compensate the WF distortions.

A particular type of AO systems is the ground layer adaptive optics (GLAO), which relies on the correction of the lowest layers of the atmospheric turbulence to improve the image quality delivered to astronomical observations. A practical implementation of this type of AO faces numerous difficulties. Indeed, in contrast with classical on-axis AO, GLAO requires excluding the highest layers of the atmosphere from the correction brought by the system. This can be done by using *i*) Rayleigh guide-star, for limited telescope diameters, or *ii*) with multiple Na-Laser guide star, for



larger telescopes. The combination of powerful laser sources at the Na wavelength and low noise fast detectors makes possible today to implement GLAO systems on 8-m-class telescope.

### 3.2 Design of the module

GRAAL is a wide FoV GLAO system developed for an 8-m class telescope, with a free-from optics scientific FoV of over  $10.5'$ . Its sky coverage exceeds 95%, and allows 100% sky coverage with a slightly limited performance. GRAAL offers an improvement of about 40% on the K-band FWHM, allowing routine observations with  $0.3''$  FWHM (50% of the time with a seeing in the line of sight of  $0.95''$ ). This represents a factor 2 with respect to the current situation, where worse seeing conditions are used more often by HAWK-I than by the AO instruments MUSE (in narrow field mode) and SINFONI, located on other foci of the same telescope. It also allows using the full potential of HAWK-I and its sampling of  $0.1''$  per pixel.

The UTs of the Paranal observatory have been designed such as to minimize the non-atmospheric sources of image degradation, with for instance a closed-loop active optics during science observations. GRAAL therefore only corrects further these disturbances at higher temporal frequencies, excepted in the case of very good seeing, where the telescope and enclosure residual seeing contributions might become significant in the PSF formation. GRAAL is based on a 4 Na-LGS (sodium

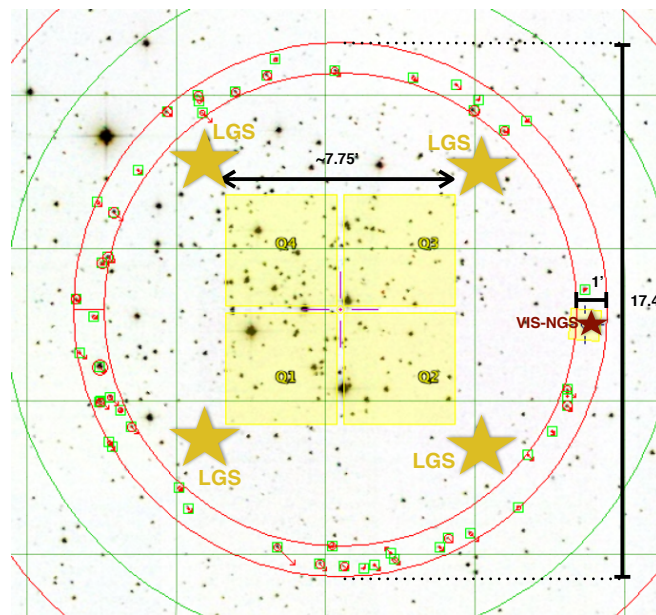


Figure 5: GRAAL focal plane illustration. The 4 LGS rotate with respect to the FoV and the lasers are side-launched. The visible TT-star selection annuli is shown. **However, HAWK-I is offered in TTS-free mode only. So users can neglect that part.**

Laser Guide-Stars) system, launched from the corners of the centrepiece of UT4. As shown in Fig. 5, the lasers are pointed towards areas located outside of the science FoV ( $7.5' \times 7.5'$ ), and the light re-emitted by the 80-100 km altitude Sodium layer is collected by 4 WFS each with  $40 \times 40$  subapertures. The slopes provided by the WFS are combined to provide an estimate of the WF error for the lowest layers; this shape is then removed from the actual shape of the DSM. The AO-loop is closed at a 700 to 1000 Hz frequency.

The science HAWAII 2RG infrared sensors of HAWK-I is used to correct slow drifts between visible

WFS and IR imaging paths, coming from flexures and uncompensated atmospheric dispersion, taking the opportunity of continuous reading of the science detectors during integration.

HAWK-I uses the adapter/rotator of the Nasmyth focus to derotate its FoV. On the opposite, GRAAL LGS-WFS must derotate the pupil; therefore GRAAL includes an LGS-ring, a derotator carrying the LGS-WFS, which counteracts the adapter's effect (to which is added the pupil rotation, proportional to the elevation of the telescope). Therefore, to summarise GRAAL science mode is based on the use of:

- 4 LGS projected on-sky with the help of 4 dedicated launched telescopes
- The corresponding WFS located on a 12' diameter ring,
- truth sensing is realized by the telescope guide-probes, a 21x21 Shack-Hartmann sensor already in operation in Paranal since the telescope installation for active optics control. Note that the active optics control will be superseded by the fast AO loop, so that the active optics sensor will be blind to all modes but the ones invisible to the AO system, the first of them being the focus mode
- SPARTA, an RTC platform sharing commonalities of hardware and software design with other AO systems (GALACSI and SPHERE) and
- the DSM

### 3.3 Wavefront sensors

The LGS sensor unit consists of 4 identical systems. Each one is composed of:

- One small pick-up mirror placed with a fixed arm at 5.8'' from the optical axis on the Nasmyth focal plane
- One trombone allowing focusing on the LGS
- One re-imaging objective composed of two lenses
- One 40x40 micro lenses array
- One 240x240 L3 CCD and NGC controller

Each pick-up mirror redirects the LGS light to a classical Shack-Hartmann WFS. The system accepts focus variations from 80 to 180 km.

## Part II

# Instrument Performance

## 4 Detectors

The naming convention for the four detectors is shown in Figure 4.

Note that quadrant 1,2,3,4 are usually, **but not necessarily**, stored in extensions 1,2,4,3 of the HAWK-I FITS file. Indeed, FITS convention forbids to identify extensions by their location in the file. Instead, look for the FITS keyword EXTNAME in each extension and verify that you are handling the quadrant that you expect (e.g. EXTNAME = 'CHIP1.INT1').

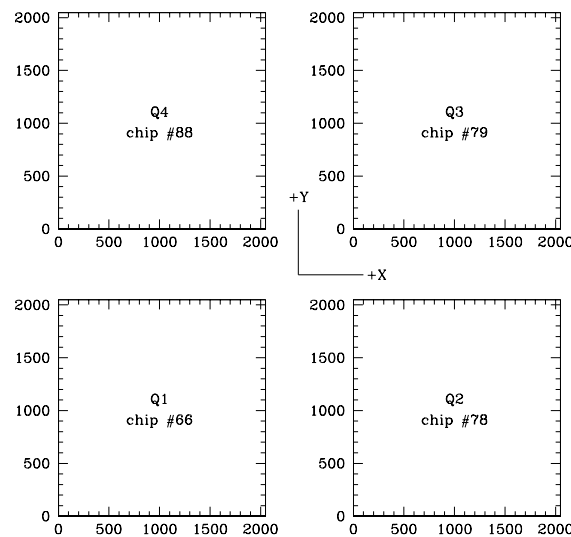


Figure 6: HAWK-I detectors naming convention

The characteristics of the four detectors are listed below:

| Detector Parameter                         | Q1                                    | Q2    | Q3    | Q4    |
|--|---------------------------------------|-------|-------|-------|
| Detector Chip #                            | 66                                    | 78    | 79    | 88    |
| Operating Temperature                      | 75K, controlled to 1mK                |       |       |       |
| Gain [e <sup>-</sup> /ADU]                 | 1.979                                 | 2.133 | 1.991 | 2.429 |
| Dark current (at 75 K) [e <sup>-</sup> /s] | between 0.10 and 0.15                 |       |       |       |
| Minimum DIT                                | 1.6762 s                              |       |       |       |
| Read noise <sup>1</sup> (NDR)              | ~ 5 to 12 e <sup>-</sup>              |       |       |       |
| Linear range (1%)                          | 60.000 e <sup>-</sup> (~ 30.000 ADUs) |       |       |       |
| Saturation level                           | between 40.000 and 50.000 ADUs        |       |       |       |
| DET.SATLEVEL                               | 25000                                 |       |       |       |

<sup>1</sup> The noise in Non-Destructive Read (NDR) depends on the DIT: the detector is read continuously every ~1.6762s, i.e. the longer the DIT, the more reads are possible and the lower the RON. For the minimum DIT

(1.6762s), the RON is  $\sim 12e^-$ ; for DIT=10s, the RON is  $\sim 8e^-$  and for DIT>15s, the RON remains stable at  $\sim 5e^-$ .

Figure 7 represents the quantum efficiency curve for each of the detectors.

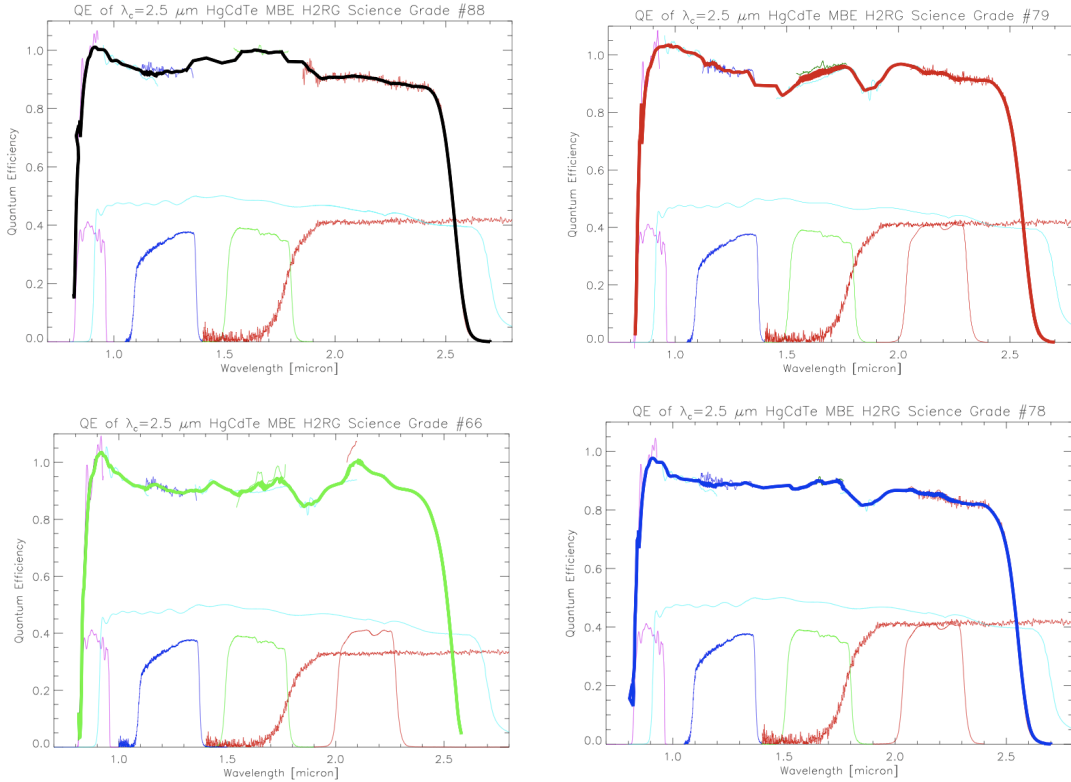


Figure 7: Quantum efficiency of the HAWK-I detectors

See appendix A for further details on the detectors features and relative sensitivity.

## 4.1 Threshold-limited integration

The normal mode of operation of the HAWK-I detectors defined a threshold by setting the keyword DET.SATLEVEL. All pixels which have absolute ADU values below this threshold are processed normally. Once pixels illuminated by a bright star have absolute ADU values above the threshold, the values are no longer used to calculate the slope of the regression fit. For these pixels only non-destructive readouts having values below the threshold are taken into account. The pixel values written into the FITS file is the value **extrapolated** to the integration time DIT and is calculated from the slope using only readouts below the threshold (Figure 8). The pixels that have been extrapolated can be identified because their values are above DET.SATLEVEL.

## 5 Field of view

The FoV of HAWK-I is defined by four Hawaii-2RG chips of  $2048^2$  pixels each (1 pixel corresponds to  $0.106''$  on the sky). The detectors are separated by gaps of about  $15''$ . Figure 9 shows how the FoV looks like.

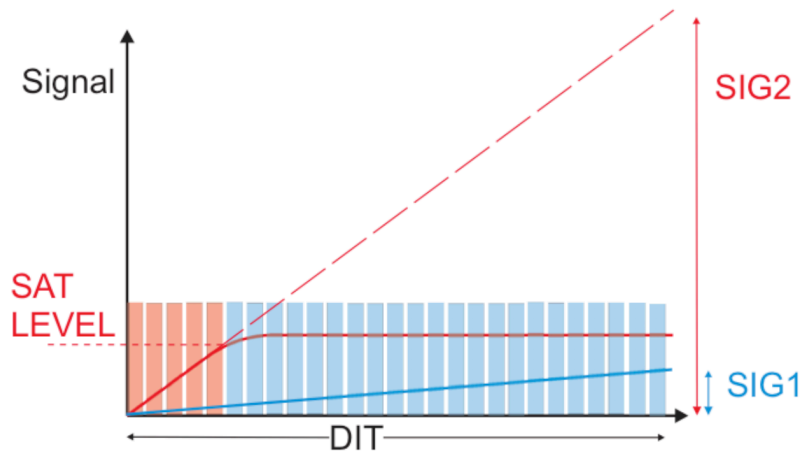


Figure 8: Saturation threshold for nondestructive sampling and extrapolation of detector signal for high flux levels. Only pixel values below SATLEVEL are taken into account for calculation of slope for pixels with high flux (red). For low flux pixels (blue) all nondestructive readouts indicated by rectangles are used.

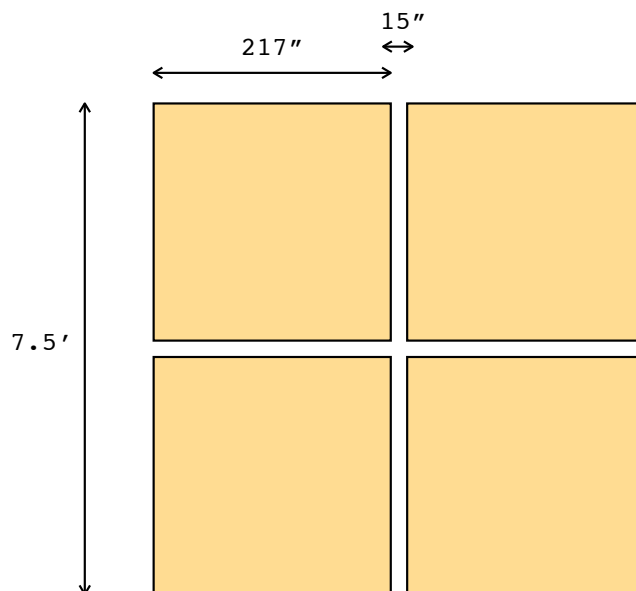


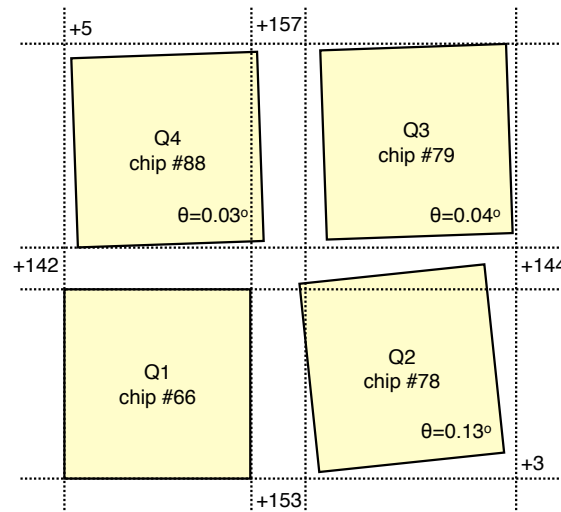
Figure 9: HAWK-I FoV

Note that it is very tempting to point *right onto* your favourite target and to loose it in the gap, since this is where the telescope points.

**BEWARE of the gap between the detectors!** And see the details in Appendix 5.

## 5.1 Relative position of the four quadrants

The four quadrants are very well aligned with respect to each other. Yet, small misalignments exist. They are sketched below:



Quadrants 2,3,4 are tilted with respect to quadrant 1 by 0.13, 0.04, 0.03 degrees, respectively. Accordingly, the size of the gaps changes along the quadrant edges.

**The default orientation (PA=0 deg) is North along the +Y axis, East along the -X axis, for quadrant #1.**

For reference purposes, we use the (partly arbitrarily) common meta system:

| Quadrant | offset in X (pix) | offset in Y (pix) |
|----------|-------------------|-------------------|
| Q1       | 0                 | 0                 |
| Q2       | 2048 + 153        | 0 + 3             |
| Q3       | 2048 + 157        | 2048 + 144        |
| Q4       | 0 + 5             | 2048 + 142        |

It is valid in its crude form to within a few pixels. The distortion corrections for a proper astrometry will be added to all image headers.

Distortions (including the obvious rotation component) will be defined with respect to the above system. First qualitative evaluations with respect to HST/ACS astrometric calibration fields recovered the relative positions of objects to about 5 mas once the distortion model was applied (a precision that should satisfy most purposes).

## 5.2 Center of Rotation and Centre of Pointing

The center of rotation of the instrument **is not exactly the centre of the detector array.**

In the standard orientation (North is +Y, East is -X) the center of the detector will be located  $\sim 0.4''$  East and  $\sim 0.4''$  South of the telescope pointing.

The common reference point for all four quadrants, taken as the centre of the telescope pointing and centre of rotation, has the following pixel coordinates (to  $\pm 0.5$  pix) in the respective quadrant reference system:

| Quadrant | CRPIX1 | CRPIX2 |
|----------|--------|--------|
| Q1       | 2163   | 2164   |
| Q2       | -37.5  | 2161.5 |
| Q3       | -42    | -28    |
| Q4       | 2158   | -25.5  |

The CRVAL1 and CRVAL2 have the on-sky coordinates of the telescope pointing (FITS keywords TEL.TARG.ALPHA , TEL.TARG.DELTA) in all quadrants.

### 5.3 Vignetting of the FoV

The Hawaii2RG detectors have 4 reference columns/rows around each device which are not sensitive to light. In addition, due to necessary baffling in the all-reflective optical design of HAWK-I, some vignetting at the edges of the field has turned out to be inevitable due to positioning tolerances of the light baffles. The measured vignetting during commissioning on the sky is summarised in the following table:

| Edge | No of columns or rows vignettted > 10% | Maximum vignetting |
|------|--|--------------------|
| +Y   | 1                                      | 14%                |
| -Y   | 8                                      | 54%                |
| -X   | 7                                      | 36%                |
| +X   | 2                                      | 15%                |

The last column represents the maximum extinction of a vignettted pixel, i.e. the percentage of light absorbed in the pixel row or column, with respect to the mean of the field.

Note : although the +Y edge vignetting is small in amplitude, it extends to around 40 pixels at < 10%.

## 6 Filters

HAWK-I is equipped with 10 filters: 4 broad band filters, and 6 narrow band filters. Please refer to appendix B for detailed characteristics and the URL to download the filter curves in electronic form.

The broad-band filters are the classical NIR filters: Y,J,H,Ks. The particularity of HAWK-I is that the broad band filter set has been ordered together with the ones of VISTA. They are thus *identical* which allows easy cross-calibrations and comparisons.

The narrow band filters include 3 cosmological filters (for Ly $\alpha$  at  $z$  of 7.7 ( $1.06\mu\text{m}$ ) and 8.7 ( $1.19\mu\text{m}$ ), and H $\alpha$  at  $z = 2.2$ , i.e.  $2.09\mu\text{m}$ ) as well as 3 stellar filters (CH $_4$ , H $_2$ , Br $\gamma$ ).

Since P113, HAWK-I filter wheel#2 is not fully functional. For this reason we have only limited availability of the narrow band filters. If you plan to use any of the narrow band filters, please submit a ticket to the ESO User Support Department via <https://support.eso.org> well before the proposal deadline.

The transformations from the 2MASS magnitudes ( $J_{2MASS}$ ,  $H_{2MASS}$ , and  $K_{2MASS}$ ) to the magnitudes in the HAWK-I filters (Y, J, H, K<sub>s</sub>, CH4, H2, BrG, NB1060, NB1190, and NB2090) are as follows:

$$\begin{aligned}
 Y &= 1.52 * J_{2MASS} - 0.52 * H_{2MASS} \\
 J &= 0.85 * J_{2MASS} + 0.15 * H_{2MASS} \\
 H &= 0.06 * J_{2MASS} + 0.94 * H_{2MASS} \\
 K_s &= 0.03 * J_{2MASS} + 0.97 * K_{2MASS} \\
 CH4 &= 0.06 * J_{2MASS} + 0.94 * H_{2MASS} \\
 H2 &= 0.03 * J_{2MASS} + 0.97 * K_{2MASS} \\
 BrG &= 0.03 * J_{2MASS} + 0.97 * K_{2MASS} \\
 NB1060 &= 1.50 * J_{2MASS} - 0.50 * H_{2MASS} \\
 NB1190 &= 0.85 * J_{2MASS} + 0.15 * H_{2MASS} \\
 NB2090 &= 0.03 * J_{2MASS} + 0.97 * K_{2MASS}
 \end{aligned}$$

Can you bring your own filters? Possibly.

HAWK-I hosts large (105mm<sup>2</sup>, i.e. expensive) filters, and was designed to have an easy access to the filter wheel. However, to exchange filters the instrument needs to be warmed up, which is not possible at any time during the year, but is scheduled on a year-by-year basis, in a way that a new filter can be installed only during regular instruments warming and maintenance (every 18 months).

At least 3 months before the proposal deadline, interested users must contact the ESO User Support Department via <https://support.eso.org> to indicate their desire to submit a proposal which would require installing a visitor filter. They will then be informed if it possible at all and the timescale involved.

## 7 Limiting magnitudes

Limiting magnitudes are of course very much dependent on the observing conditions. The [exposure time calculator](#) (ETC) is reasonably well calibrated and we strongly encourage you to use it. In order to give you a rough idea of the performance to be expected for NoAOF mode observations, we list here the limiting magnitudes (S/N=5 for a point source in 3600s integration on source) under average conditions (0.8" seeing, 1.2 airmass):

| Filter         | Limiting mag<br>[Vega] | Limiting mag<br>[AB] | Saturation limit<br>(in 2 sec) |
|----------------|------------------------|----------------------|--------------------------------|
| J              | 23.9                   | 24.8                 | 10.0                           |
| H              | 22.5                   | 23.9                 | 10.3                           |
| K <sub>s</sub> | 22.3                   | 24.2                 | 9.2                            |

Under the same average conditions (0.8" seeing, 1.2 airmass), HAWK-I in combination with GRAAL reaches, for the same integration time, 0.2 mag fainter point sources at the same S/N than without correction.



For more detailed exposure time calculation, in particular for narrow band filters, please use the [exposure time calculator](#).

As for persistence on HAWKI detectors, the following rules apply. When using DITs smaller than 30 secs, persistence effects can be neglected. However, when using larger DITs the maximum accepted saturation is 7 times the HAWKI saturation level. Therefore, users are recommended to check carefully their fields against saturation using HAWKI ETC during Phase II and, in case, submit a [waiver](#), which will be evaluated on individual case basis.

## 8 Image quality and astrometry

The image quality of HAWK-I is excellent across the entire field of view. In seeing limited mode (No-AOF) distortions are below 2% over the full 10' diagonal and the image quality has always been limited by the seeing (our best recorded images had FWHM below 2.2 pix, i.e.  $<0.23''$  in the Ks band). A reduction of the PSF FWHM by a factor of at least 1.25 is achieved when HAWK-I is used in combination with GRAAL. The FWHM improvement factor highly depends on the ground layer fraction measured at the moment of the information, as seen in the Figure 10. It is highly recommended to use the HAWK-I ETC to determine what the turbulence category needs to be requested to achieve the required image quality for the scientific goal. In November 2021, the HAWK-I 3LGS mode is commissioned. The 3LGS mode could be used, when one of the lasers is out of operation. The performance of degraded 3LGS mode is very similar to that of full 4LGS mode.

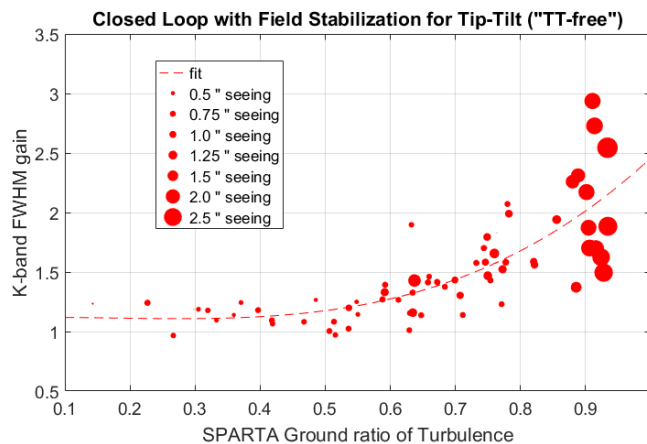


Figure 10: FWHM gain in Ks-band in function of the DIMM seeing and the ground layer fraction measured in TTS-free mode.

The photometric accuracy and homogeneity that we measured across one quadrant is  $<5\%$  (as monitored on 2MASS calibration fields). We expect that with an even more careful illumination correction and flat-fielding about 3% absolute accuracy across the entire field will be achieved routinely when the calibration database is filled and stable. This is still valid for GRAAL+HAWK-I observations.

Of course, differential photometry can be pushed to a higher accuracy. Note in particular, that given the HAWK-I field size, between 10 and 100 useful 2MASS stars (calibrated to 0.05 – 0.10 mag) are usually present in the field.

Finally, the relative astrometry across the entire field is auto-calibrated on a monthly basis (see HAWKI calibration plan), using a sample of globular clusters as references. The distortion map currently allows to recover relative position across the entire field with a precision of  $\sim 0.1''$ , which is still true with GRAAL.

A note of caution: as all current infrared arrays, the HAWK-I detectors suffer of persistence at the level of  $10^{-3} - 10^{-4}$  (depending on how badly the pixels were saturated) that decays slowly over minutes (about 5min for the maximum tolerated saturation level in SM). This might leave artefacts reflecting the dither pattern around saturated stars.

## Part III

# Observing with HAWK-I: from phase 1 to data reduction

This part of the document helps you to decide whether HAWK-I is the right instrument for your scientific project, and it provides guidelines for Phase 1 and Phase 2 preparation.

**Important change from P105:** the previous Seeing Constraint now is replaced by a Turbulence Category. For HAWKI no-AO mode, the Turbulence Categories are defined using the percentiles of the zenith V-band seeing distribution as follow:

Table 1: Acquisition and science HAWK-I templates

| Turbulence Category | 10%  | 20%  | 30%  | 50%  | 70%  | 85%  | 100% |
|---------------------|------|------|------|------|------|------|------|
| Seeing threshold    | 0.5" | 0.6" | 0.7" | 0.8" | 1.0" | 1.3" | all  |

A image quality gain is expected when HAWK-I is used in combination with GRAAL in the ground layer AO mode. The gain depends on the ground layer fraction, and please refer to the ETC to select the turbulence category that is required to match the desired image quality on the image.

## 9 Introduction

HAWK-I performs direct imaging in the NIR (0.97 to 2.31  $\mu\text{m}$ ) over a FoV of  $7.5' \times 7.5'$ , with a pixel scale of 0.106" per pixel. The basic characteristics of the instrument are summarised in the nutshell at the beginning of this document, whereas details on the instrument performance can be found in Part II.

HAWK-I can be used in seeing limited mode or in combination with GRAAL, which is a seeing improver allowing to enhance the instrument image quality. In particular, the following two operational modes are offered:

- AOF TTS-free: This mode allows the setup of the instrument without a TTS, hence it can be realised via the LGS only;
- no-AOF: In this case GRAAL is not used and the observation are performed in seeing limited mode.

## 10 Phase 1: applying for observing time with HAWK-I

Now that you have decided that HAWK-I is the right instrument to carry on your science project you must apply for observing time. To do that properly there is a number of details that you must take into account ahead in time, and this section will guide you through it.

## 10.1 Getting reasonable photometry with HAWK-I

If good photometry is your goal, you should go for one of the following options.

- **Ask for special calibrations!** Take into account as early as Phase 1 (i.e. in your proposal) the fact that you want to observe more and/or other standard fields than the ones foreseen in the calibration plan.

In your README file you can then explain that you want your specified standard field observed e.g. before and after your science OB. Use an OB concatenation if you want to observe a standard in immediate sequence with your science target.

You can also specify that you want illumination maps for your filters close in time to your observations, and/or specify as special calibrations your own illumination maps.

- If a photometric calibration to  $\sim 0.05$ – $0.1$  magnitude is enough for your program, consider that the HAWK-I field is large and that (by experience) you will have 10–100 stars from the 2MASS catalog in your field.

These are typically cataloged with a photometry good to  $< 0.1$  mag and would allow to determine the zero point on your image to  $\sim 0.05$  mag, using these "local secondary standards". Extinction coefficients would automatically be taken into account. They are measured on a monthly basis. Besides, we remind that colour terms for HAWK-I are small,  $\sim 0.1 \times (J-K)$ .

**Check with Skycat (or Gaia) ahead of time whether good (non-saturated!) 2MASS stars are present in your science field.**

Skycat is available under <http://archive.eso.org/skycat/>

Gaia is part of the starlink project: <http://starlink.jach.hawaii.edu/>

### 10.1.1 Consider the 2MASS calibration fields

The 2MASS mission used a number of calibration fields for the survey. Details are given at [http://www.ipac.caltech.edu/2mass/releases/allsky/doc/seca4\\_1.html](http://www.ipac.caltech.edu/2mass/releases/allsky/doc/seca4_1.html)

In particular the sect.III, 2 [http://www.ipac.caltech.edu/2mass/releases/allsky/doc/sec3\\_2d.html](http://www.ipac.caltech.edu/2mass/releases/allsky/doc/sec3_2d.html) provides a list of fields (touch-stone fields) that you could use as photometric fields in order to calibrate your observations.

### 10.1.2 HAWK-I extinction coefficients

We measured HAWK-I extinction coefficient for the broad-band filters as a result of a year monitoring. The results are:

$$J = 0.043 \pm 0.005$$

$$H = 0.031 \pm 0.005$$

$$K_s = 0.068 \pm 0.009$$

$$Y = 0.021 \pm 0.007$$

We plan to keep monitoring these coefficients on a monthly basis, according to the calibration plan.

## 10.2 The Exposure Time Calculator

The HAWK-I ETC returns a good estimation of the integration time (on source!) needed in order to achieve a given S/N, as a function of atmospheric conditions.

A few words about various *input variables* that might not be quite standard (also read the online help provided on the ETC page):

- The input magnitude can be specified for a point source, for an extended source (in which case we compute an integration over the surface defined by the input diameter), or as surface brightness (in which case we compute values per pixel e.g.  $106 \times 106$  mas).
- The user can provide as input parameter either the Turbulence Category, or the desired image quality (IQ) at the observing wavelength. In the latter case the ETC will return the corresponding value for the Turbulence Category, which is the relevant parameter to be specified at Phase I.
- Among the instrument set-up parameters needed as input for the ETC, the mode is very important. You need to specify whether the simulation should be run with or without GRAAL.
- The level of precipitable water vapour (PWV) can make impact on the atmospheric transmission of the near-IR light. Figure 11 shows the effect of PWV in different near-IR bands. The PWV will make about 5% to 15% impact on the total transmission depending the filter band and PWV value. Please refer to Figure 11 and HAWK-I ETC for more details.
- Results are given as exposure time to achieve a given S/N or a S/N achieved in a given exposure time. In both cases, you are requested to input a typical DIT, which for broad band filters will be short (10 to 30s) but for narrow band filters could be long exposures between 60 and 300s before being sky background limited.
- Do not hesitate to make use of the many graphical outputs. In particular for checking your target line (and the sky lines) in the NB filters...

The *screen output from the ETC* will include the input parameters together with the calculated performance estimates. Here some additional notes about the ETC output values:

- The integration time is given on source: depending on your technique to obtain sky measurements (jitter? or offsets?), and accounting for overheads, the total observing time will be much larger.
- The S/N is computed over various areas as a function of the source geometry (point source, extended source, surface brightness). Check carefully what was done in your case.

Most of the other ETC parameters should be self-explaining and/or well explained in the online help of the ETC.

## 10.3 Proposal Form

Your proposal must be submitted by the respective deadline (end of March and end of September). Since DDT proposals during period 103, and all proposals for P105, the User is required to create the proposal using the new web based Phase 1 tool ([www.eso.org/p1](http://www.eso.org/p1)). Using this tool, the

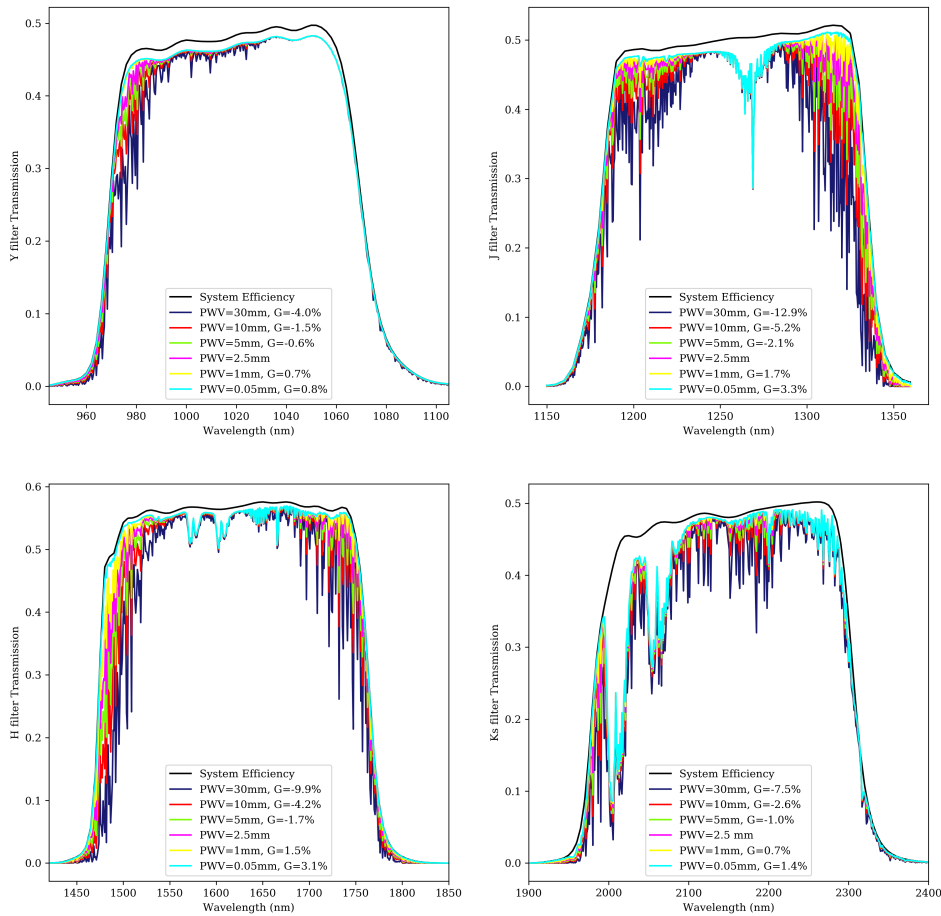


Figure 11: Effect of PWV on the transmission curves of Y-, J-, H-, and K-bands. The black curves denote the transmission curve without atmosphere effects, and the color curves represent the transmission curve convolved with the sky transmission at different PWV values. PWV=2.5mm is used as a reference value to compute the G (GAIN) value in the different PWV values.

User creates a proposal and Phase 1 materials adding the scientific rationale and other relevant information. In this Phase 1 tool the User creates the observing runs, chooses instrument, modes, observing constraints, and adds the targets to each defined run.

Finally, the seeing condition to be requested at Phase I refers to Turbulence Category, therefore you must enter the value used by the ETC simulations.

### 10.4 Overheads and Calibration Plan

When applying for HAWK-I, do not forget to take into account all the overheads when computing the required time.

- Make sure that you compute the exposure time including on sky time (not only on source) if your observing strategy requires it.
- Verify in the [call for proposal](#) that you have taken into account all listed overheads; which can also be found in Sect. [12.6](#). To do so you can either refer to Sect. [12.6](#) or simulate the detailed breakdown of your program in terms of its constituent Observing Blocks (OBs) using the p2 tutorial account ([p2 tutorial](#)).

The Execution Time Report option offered by p2 provides an accurate estimate of the time needed for the execution of each OB, including all necessary overheads.

- Check whether you need any special calibration: have a look at the calibration plan in Sect. [C](#) – this is what the observatory will give you as default. You might need more, and we will be happy to provide you with more calibrations, if you tell us in advance which. Note however that night calibrations should be accounted for by the user. Any additional calibration you might need should be mentioned in the Phase 1 proposal and the corresponding (night) time to execute them must be included in the total time requested.

## 11 Phase 2: preparing your HAWK-I observations

All scientific and calibration observations with HAWK-I are prepared by OBs as a sequence of the available templates. This is performed with the help of the phase 2 proposal preparation tool (web-based p2 application).

This sections provides a preliminary guide for the observation preparation for HAWK-I in Phase 2, both for SM or VM.

We assume that you are familiar with the existing generic guidelines:

- [Proposal preparation](#)
- [SM informations](#)
- [VM informations](#)

We know that they are not super-thrilling, but a quick browse over them might save you some time during Phase 2.

### 11.1 HAWK-I specifics to templates, OBs, and p2

HAWK-I follows very closely the philosophy set by the ISAAC (short wavelength) and NACO imaging templates.

#### 11.1.1 HAWKI p2

Using [p2](#) to prepare HAWK-I observations does not require any special functions. Indeed, for no-AOF and TTS-free mode no file has to be uploaded, except for the finding chart (see section [11.1.4](#)) and possibly ephemerides, because all other entries are typed.

Step by step tutorial on how to prepare OBs for HAWK-I with p2 can be found [here](#) .

#### 11.1.2 Observing Blocks – OBs

Any HAWK-I science OB should contain one acquisition template, followed by a number of science templates.

If this **did** surprise you, you may need to get [back to the basics](#).

#### 11.1.3 Templates

The HAWK-I templates are described in detail in the template reference guide available through the [instrument web pages](#).

A brief overview is given below. If you are familiar with the ISAAC SW imaging or NACO imaging templates, these will look very familiar to you and cover essentially the same functionalities.

The acquisition and science templates are listed in [Table 2](#).

Two kinds of acquisition exist, that is a simple preset with no possibility to interactively place the target in a given position on the detector and an interactive acquisition where a target can be moved to a specified position. Also, each instrument mode has a dedicated acquisition template.



The science templates provide three forms of obtaining sky images: small jitter patterns for uncrowded fields; fixed sky-offsets for extended or crowded fields when the off-position needs to be acquired far from the target field; and finally the possibility to define an arbitrary offset pattern, when the standard strategies are not suited. Note that, unlike the acquisition, the science templates do not depend on whether or not GRAAL is used.

For Rapid Response Mode (RRM) we have only one dedicated acquisition template, which is exactly the same as the one for noAOF observations, but with the string RRM appended to the name. RRM observation are only allowed without GRAAL (i.e. in No-AOF mode).

Table 2: Acquisition and science HAWK-I templates

| acquisition templates          | functionality                              | comment                              |
|--------------------------------|--|--------------------------------------|
| HAWKI_img_acq_Preset           | Simple telescope preset                    | For observation in no-AOF mode       |
| HAWKI_img_acq_PresetRRM        | Simple telescope preset                    | For RRM observation in no-AOF mode   |
| HAWKI_img_acq_LGS_PresetRRM    | Simple telescope preset                    | For RRM observation in TTS-free mode |
| HAWKI_img_acq_LGS_Preset       | Simple telescope preset                    | For observation in TTS-free mode     |
| HAWKI_img_acq_MoveToPixel      | Interactive target acquisition             | For observation in no-AOF mode       |
| HAWKI_img_acq_MoveToPixelRRM   | Interactive target acquisition             | For RRM observation in no-AOF mode   |
| HAWKI_img_acq_LGS_MoveToPixel  | Interactive target acquisition             | For observation in TTS-free mode     |
|                                |  |                                      |
| HAWKI_img_acq_FastPhot         | Acquisition for windowed mode              | For observation in no-AOF mode       |
| HAWKI_img_acq_LGS_FastPhot     | Acquisition for windowed mode              | For observation in TTS-free mode     |
| HAWKI_img_acq_FastPhotRRM      | Acquisition for windowed mode              | For RRM observations in no-AOF mode  |
| science templates              |  |                                      |
| HAWKI_img_obs_AutoJitter       | imaging with jitter (no offsets)           | recommended for low-density fields   |
| HAWKI_img_obs_AutoJitterOffset | imaging with jitter and random sky offsets | recommended for extended objects     |
| HAWKI_img_obs_FixedSkyOffset   | imaging with jitter and fixed sky offsets  | when random sky is not suited        |
| HAWKI_img_obs_GenericOffset    | imaging with user defined offsets          |                                      |
| HAWKI_img_obs_FastPhot         | imaging with fast read out and windowing   |                                      |

The calibration and technical templates are listed in Table 3.

The only calibration template accessible to the SM user is the one to take standard stars.

The calibration templates are foreseen to acquire darks, flat-fields and simple standard star observations to calibrate the zero point (the latter only in noAOF mode).

The technical templates are used for the periodical characterisation of the instrument. The illumination frames are used to determine the variation of the zero point as a function of detector position. The astrometry and flexure templates are needed to compute the distortion map, the plate scale and relative positions of the detectors and to quantify possible flexures. Three further templates are used to characterise the detector, to determine the best telescope focus and to measure the reproducibility of the filter wheel positioning.

#### 11.1.4 Finding Charts and README Files

A Finding Chart Generation service called p2fc is integrated into p2. To use the p2fc service, in p2 just select the OB(s) and then click the 'Generate Finding Chart(s)' button, finding charts will then be added to the OB(s), provided there is space for them (up to 5 finding charts can be added to any OB, so there needs to be at least 2 slots free or already occupied by charts generated by the p2fc service – note p2fc will replace any p2fc generated finding charts already attached to the OB).

The general instructions on the README files that are available at:

Table 3: Calibration and technical HAWK-I templates

| calibration templates      | functionality                                   | comment                  |
|----------------------------|---|--------------------------|
| HAWKI_img_cal_Darks        | series of darks                                 |                          |
| HAWKI_img_acq_TwPreset     | acquisition for flat-field                      |                          |
| HAWKI_img_cal_TwFlats      | imaging twilight flat-field                     |                          |
| HAWKI_img_cal_SkyFlats     | imaging sky flat-field                          |                          |
| HAWKI_img_cal_WinTwFlats   | windowed imaging twilight flat-field            |                          |
| HAWKI_img_cal_WinSkyFlats  | windowed imaging sky flat-field                 |                          |
| HAWKI_img_cal_StandardStar | no-AOF imaging of standard field                | available to the SM user |
| technical templates        |   |                          |
| HAWKI_img_tec_IlluFrame    | imaging of illumination field                   |                          |
| HAWKI_img_tec_Astrometry   | imaging of astrometric field                    |                          |
| HAWKI_img_tec_Flexure      | measuring instrument flexure/center of rotation |                          |
| HAWKI_img_tec_DetLin       | detector test/monitoring                        |                          |
| HAWKI_img_tec_Focus        | telescope focus determination                   |                          |
| HAWKI_img_tec_FilterWheel  | filter wheel positioning accuracy               |                          |
| HAWKI_img_tec_switchMODE   | to change the instrument mode                   |                          |

<http://www.eso.org/sci/observing/phase2/SMGuidelines/ReadmeFile.generic.html>,

The following HAWK-I specific is recommended: The (IR) magnitude of the brightest star in the field must be specified in the P2 comment field of the OB.

### 11.1.5 ObsPrep tools

The ObsPrep tab of p2 allows interactive planning of the observations, e.g. the fine-tuning of the science field pointing, the selection of blind offset stars, and/or the selection of VLT guide stars. The choices made are directly reflected by an update of the respective parameters in the OB acquisition template, the science templates, and the target tab. Note that the target tab must be filled in and an acquisition template in the Obs Description tab has to be chosen before ObsPrep can be used.

A short video tutorial of ObsPrep is available [here](#).

### 11.1.6 ESO Phase 2 API

ESO has released a Phase 2 Application Programming Interface (API) that can be used to create, modify, or delete observation blocks (OBs), containers and an accompanying ReadMe file that define an observing run. In short, the API uses the lightweight JavaScript Object Notation (JSON) standard as data format to exchange information between the user-dedicated application and the Phase 2 server at ESO.

Please find more details on the ESO Phase 2 API at [here](#)

## 12 Observing strategies with HAWK-I

### 12.1 Overview

As with all other Paranal instruments, users prepare their observations with the p2 web-tool. Acquisitions, observations and calibrations are coded via templates and OBs. OBs contain all the information necessary for the execution of an observing sequence.

At the telescope, OBs are executed by the instrument operator. HAWK-I and the telescope are setup according to the contents of the OB.

The HAWK-I Real Time Display (RTD) is used to view the raw frames. During acquisition sequences, the RTD can be used as well as for the interactive centring of the targets in the field.

Calibrations including darks, sky-flats, photometric standard stars, illumination maps etc are acquired by the Observatory staff according to the calibration plan and monitored by the Quality Control group of ESO Garching.

### 12.2 Visitor Mode Operations

Information/policy on the Visitor Mode operations at the VLT are described at:

[http://www.eso.org/paranal/sciops/VA\\_GeneralInfo.html](http://www.eso.org/paranal/sciops/VA_GeneralInfo.html)

Visitors should be aware that about 30 minutes/night (of night time!) may be taken off their time, in order to perform the HAWK-I calibrations according to the calibration plan. In Visitor mode is also possible to observe bright objects using BADA0, say switching active optics off. **Telescope defocussing is however not permitted.**

### 12.3 The influence of the Moon

Moonlight does not noticeably increase the background in the NIR, so there is no need to request dark or grey time.

However, it is recommended not to observe targets closer than 30 deg to the Moon to avoid problems linked to the telescope guiding/active optics system. The effect is difficult to predict and to quantify as it depends on too many parameters. Just changing the guide star often solves the problem.

Visitors should check their target positions with respect to the Moon at the time of their scheduled observations (e.g. with the tools available at <http://www.eso.org/sci/observing/tools.html>). Backup targets are recommended whenever possible, and you are encouraged to contact [ESO](#) in case of severe conflict (i.e. when the distance to the Moon is smaller than 30 deg).

### 12.4 Twilight

Because HAWK-I is an infrared imager, observations of bright objects in no-AOF or TTS-free modes may be carried out in twilight. From P91 onwards, there is a new OB constraint in p2 called twilight constraint. This constraint can be used to define the earliest time with respect to the end of the astronomical twilight when the execution of the OB can be started. While the relation between the time difference from the evening twilight end and sun elevation varies during the year, for Paranal due to its low latitude this difference is small. Therefore the constraint is given in minutes as a

difference in time with respect to the end of astronomical twilight (i.e. the time when the solar elevation is -18 degrees). The default value of twilight constraint is -30. A negative number means that it is allowed to start the observation before the end of the astronomical twilight. The twilight constraint can take values between -45 and 0 minutes.

### 12.5 Orientation, offset conventions and definitions

HAWK-I follows the standard astronomical offset conventions and definitions: North is up and East to the left.

**All offsets are given as telescope offsets** (i.e. your target moves exactly the other way) in arc-seconds. The reference system can be chosen to be the sky (offsets 1 and 2 refer to offsets in Alpha and Delta respectively, independently of the instrument orientation on the sky) or the Detector (offsets 1 and 2 refer to the detector +X and +Y axis, respectively).

For jitter pattern and small offset, it is more intuitive to *use the detector coordinates* as you probably want to move the target on the detector, or place it on a different quadrant (in which case, do not forget the 15" gap!).

The sky reference system is probably only useful when a fixed sky frame needs to be acquired with respect to the pointing.

For a position angle of 0, the reconstructed image on the RTD will show North up (+Y) and East left (-X). The positive position angle is defined from North to East (see Fig. 12).

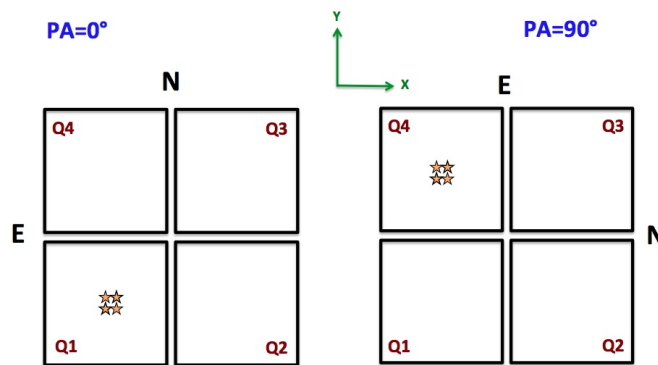


Figure 12: Definition of position angle.

Note that **the templates use always offsets relative to the previous pointing**; not relative to the *original* position (i.e. each offset is measured with respect to the *currents pointing*).

For example, if you want to place a target in a series of four offsets in the center of each quadrant: point to the star, then perform the offsets (-115,-115) [telescope moves to the lower right, star appears in the upper left, i.e. in Q4]; (230, 0); (0, 230); (-230, 0).

Note that HAWK-I offers during execution a display that shows, at the start of a template, all the offsets to be performed (see below). It provides a quick visual check whether your pattern looks as expected (see left panel of Fig. 13):

In the above example (Fig. 13, left panel) , 7 offsets are requested, and the way they are performed is shown in the right panel of Fig. 13. The sequence of offset will be: (10,10), (90,-10),(-100,200), (100,-200), (-300,420) and (580,-10).

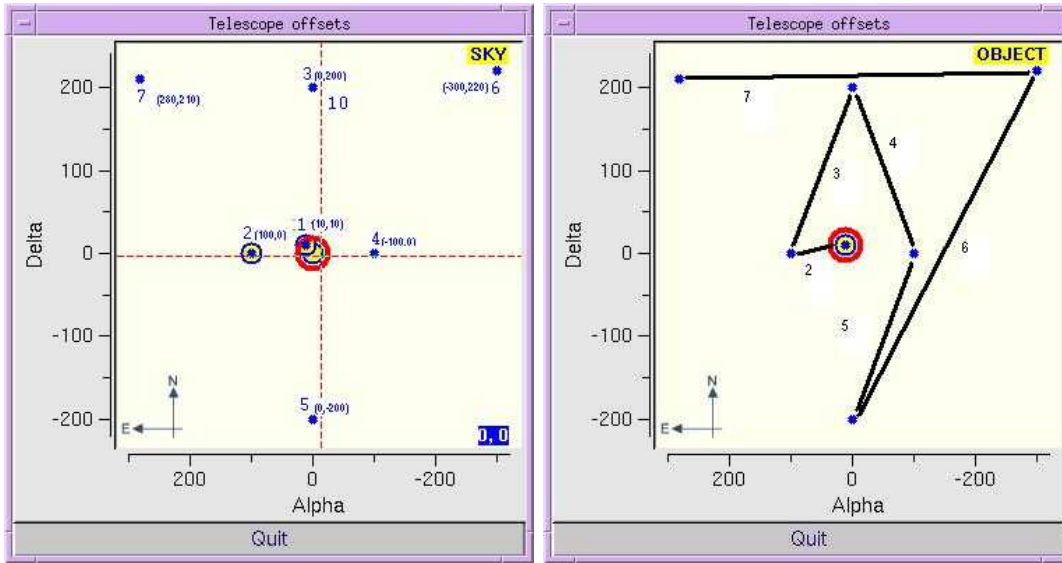


Figure 13: Left: Pop-up window at the start of an example template: it provides a quick check of your offset pattern. Right: Offset execution along the template.

### 12.6 Instrument and telescope overheads

The telescope and instrument overheads are summarised below.

| Hardware Item      | Action                                     | Time (minutes)    |
|--------------------|--|-------------------|
| Paranal telescopes | Preset                                     | 6                 |
| HAWK-I             | Acquisition NoAOF                          | ~ <sup>1</sup>    |
| HAWK-I             | Acquisition TTS-free                       | 2.6               |
| HAWK-I             | Initial instrument setup (for ACQ only)    | 1                 |
| HAWK-I             | Telescope Offset <sup>a</sup> (small)      | 0.15              |
| HAWK-I             | Telescope Offset <sup>a</sup> (large >90") | 0.75              |
| HAWK-I             | Readout (per DIT)                          | 0.03              |
| HAWK-I             | After-exposure (per exposure)              | 0.13 <sup>2</sup> |
| HAWK-I             | Filter change                              | 0.35              |

1 The instrument set-up is usually absorbed in the telescope preset for a simple preset.  
 2 The after-exposure overhead includes the readout and file merging and saving time after each exposure.

### 12.7 Recommended DIT/NDIT and Object–Sky pattern

For DITs longer than 120sec, the SM user has to use one of the following DIT: 150, 180, 240, 300, 600 and 900sec. Table 4 lists the contribution of the sky background for a given filter and DIT. Please note that these values are indicative and can change due to sky variability especially for H band, whose flux for a given DIT can fluctuate by a factor of 2, due to variations of the atmospheric OH lines. This effect also impacts the Y, J & CH4 filters. The Moon has an effect on the sky background, especially for the NB1060 and NB1190 filters. Similarly the variation of the outside temperature impacts the sky contribution for the K<sub>s</sub>, BrG, H2 and NB2090 filters. Due to the sky variations and in order to allow for proper sky subtraction, we recommend to offset at least every 2 minutes. Please be reminded that the minimum time at a position before an offset is about 1 minute.

Table 4: Sky background contribution and useful integration times.

| Filter              | Contribution from sky<br>(electrons/sec) | RON limitation<br>~DIT (sec) | linearity limit<br>~DIT (sec) | Recommended DIT<br>(sec) |
|---------------------|--|------------------------------|-------------------------------|--------------------------|
| Broad band filters  |  |                              |                               |                          |
| K <sub>s</sub>      | 1600                                     | < 1                          | 30                            | 10                       |
| H                   | 2900                                     | < 1                          | 20                            | 10                       |
| J                   | 350                                      | 1.15                         | 140                           | 10                       |
| Y                   | 130                                      | 3                            | 400                           | 30                       |
| Narrow band filters |  |                              |                               |                          |
| CH4                 | 1200                                     | < 1                          | 40                            | 10                       |
| NB2090              | 60                                       | 7                            | 900                           | 60                       |
| NB1190              | 3.6                                      | 110                          | 14000                         | 300                      |
| NB1060              | 3.4                                      | 120                          | 14000                         | 300                      |
| H2                  | 140                                      | 17                           | 400                           | 30                       |
| BrG                 | 180                                      | 15                           | 300                           | 30                       |

Figure 14 shows the quality of the sky subtraction as a function of pupil angle and time from the first frame. A sequence of frames in the K<sub>s</sub> band was obtained when the target was near the zenith, and the pupil was rotating by 2.45 degrees/minute. Being the VLT an alt-azimuth telescope the image rotates with respect to the pupil. This is noticed as a rotation of the diffraction spikes seeing around bright stars. The sky-subtraction error is larger when the pupil rotation angle between the two images is largest.



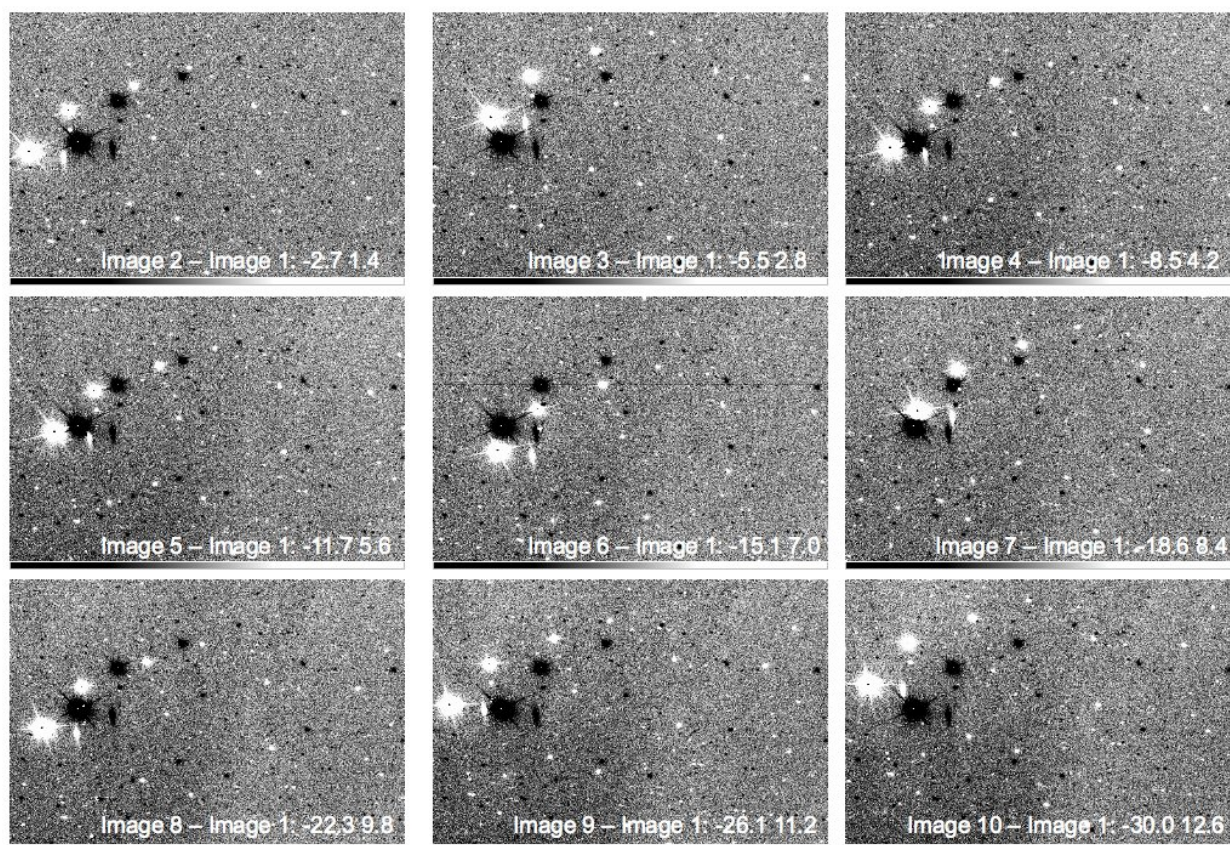


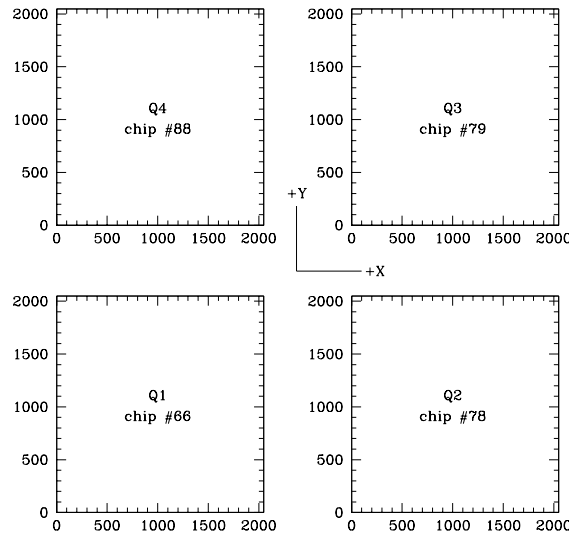
Figure 14: The annotation indicate the difference in pupil angle between the two frames being subtracted, and the difference in start time between the two exposures.

## Part IV

# Reference Material

## A The HAWK-I detectors

The naming convention for the four detectors is the following:



Note that quadrant 1,2,3,4 are usually, **but not necessarily**, stored in extensions 1,2,4,3 of the HAWK-I FITS file. Indeed, FITS convention forbids to identify extensions by their location in the file. Instead, look for the FITS keyword EXTNAME in each extension and verify that you are handling the quadrant that you expect (eg. EXTNAME = 'CHIP1.INT1').

The characteristics of the four detectors are listed below:

| Detector Parameter                 | Q1                                 | Q2    | Q3    | Q4    |
|------------------------------------|------------------------------------|-------|-------|-------|
| Detector Chip #                    | 66                                 | 78    | 79    | 88    |
| Operating Temperature              | 75K, controlled to 1mK             |       |       |       |
| Gain [ $e^-$ /ADU]                 | 1.705                              | 1.870 | 1.735 | 2.110 |
| Dark current (at 75 K) [ $e^-$ /s] | between 0.10 and 0.15              |       |       |       |
| Minimum DIT                        | 1.6762 s                           |       |       |       |
| Read noise <sup>1</sup> (NDR)      | $\sim 5$ to $12 e^-$               |       |       |       |
| Linear range (1%)                  | $60.000 e^-$ ( $\sim 30.000$ ADUs) |       |       |       |
| Saturation level                   | between 40.000 and 50.000 ADUs     |       |       |       |
| DET.SATLEVEL                       | 25000                              |       |       |       |

<sup>1</sup> The noise in Non-Destructive Read (NDR) depends on the DIT: the detector is read continuously every  $\sim 1.6762$ s, i.e the longer the DIT, the more reads are possible and the lower the RON. For the minimum DIT (1.6762s), the RON is  $\sim 12e^-$ ; for DIT=10s, the RON is  $\sim 8e^-$  and for DIT>15s, the RON remains stable at  $\sim 5 e^-$ .

Figure 15 represents the quantum efficiency curve for each of the detectors.



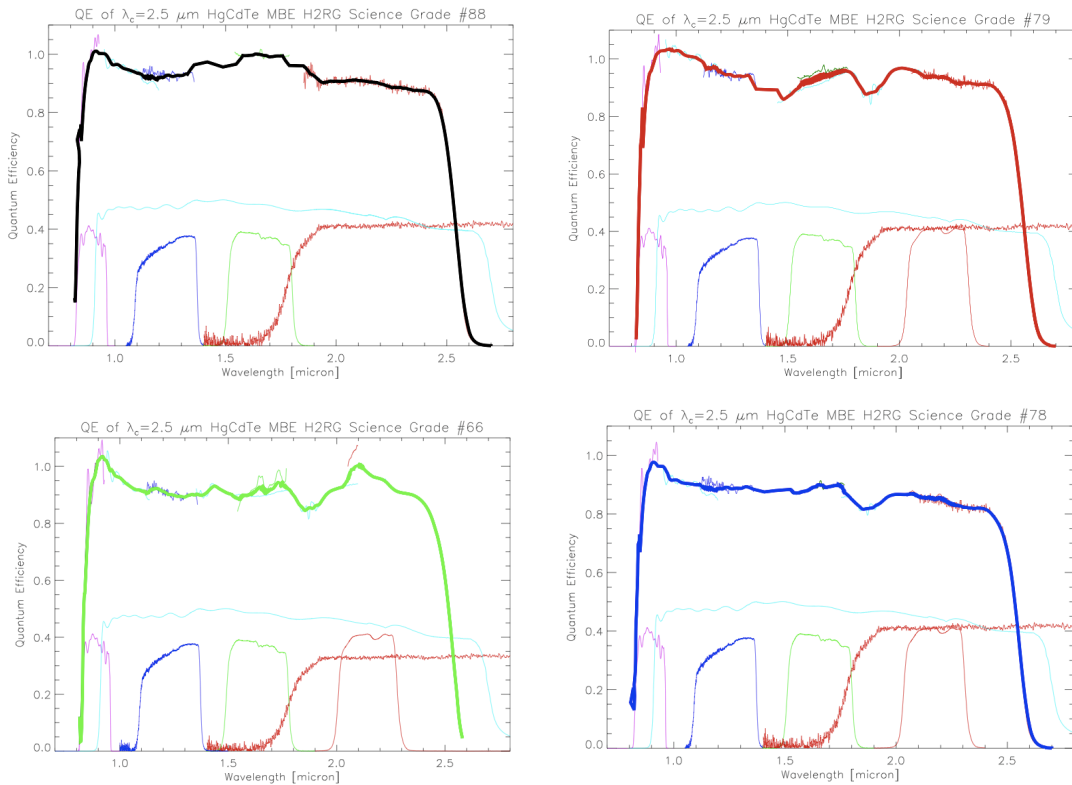


Figure 15: Quantum efficiency of the HAWK-I detectors

## A.1 Threshold-limited integration

The normal mode of operation of the HAWK-I detectors defined a threshold by setting the keyword `DET.SATLEVEL`. All pixels which have absolute ADU values below this threshold are processed normally. Once pixels illuminated by a bright star have absolute ADU values above the threshold, the values are no longer used to calculate the slope of the regression fit. For these pixels only non-destructive readouts having values below the threshold are taken into account. The pixel values written into the FITS file is the value **extrapolated** to the integration time DIT and is calculated from the slope using only readouts below the threshold. The pixels that have been extrapolated can be identified because their values are above `DET.SATLEVEL`.

## A.2 Detectors' structures and features

We present some of HAWK-I's detector features in two examples.

Figure 16 is a typical long (> 60s) exposure. Some features have been highlighted:

1. some black features on chip 66 & 79 (Q1 and Q3). For both of them, when light falls directly on these spots some diffraction structures can be seen, as shown in the corresponding quadrants in Fig. 16 .
2. On the left (chip #88) there is an artefact on the detector's surface layer. On the right (chip #79), these are sort of doughnut shaped features. More of these can be seen in Fig. 17 on chip #88. Both features are stable and removed completely by simple data reduction (no extra step needed).
3. Detector glow, which is visible for long DITs, but is removed by e.g. sky subtraction

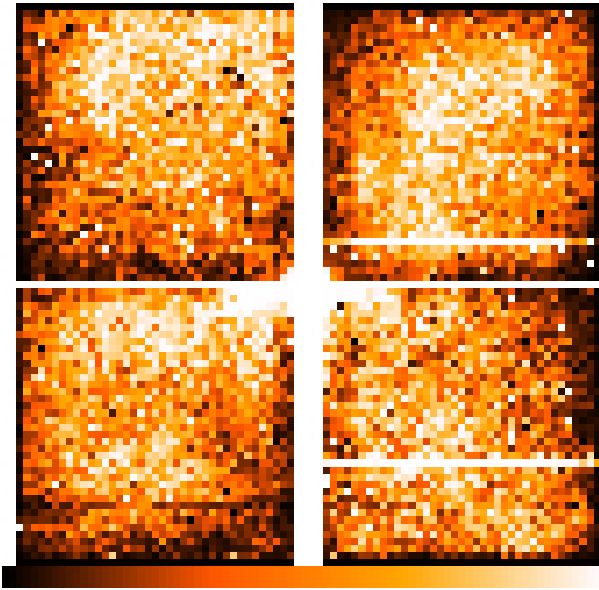


Figure 16: Typical raw HAWK-I dark frame (DIT=300sec)

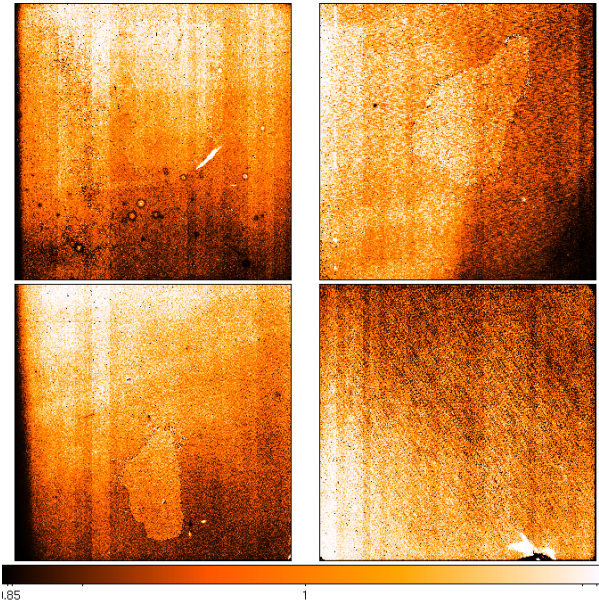


Figure 17: Typical raw HAWK-I twilight flat field (Y Band)

4. The darker area visible in Fig 16 corresponds to the shadow of the baffling between the detectors.
5. Emitting structure, whose intensity grows with the integration time. It is however fully removed by classical data reduction.
6. Q4 chip#88 dark median has been found to be larger than the other detectors, and to increase with NDIT (see Fig. 18). Thanks to Sylvain Guieu for detecting this.
7. Q2 chip#78 suffers from radioactive effects (see Fig. 19 below)

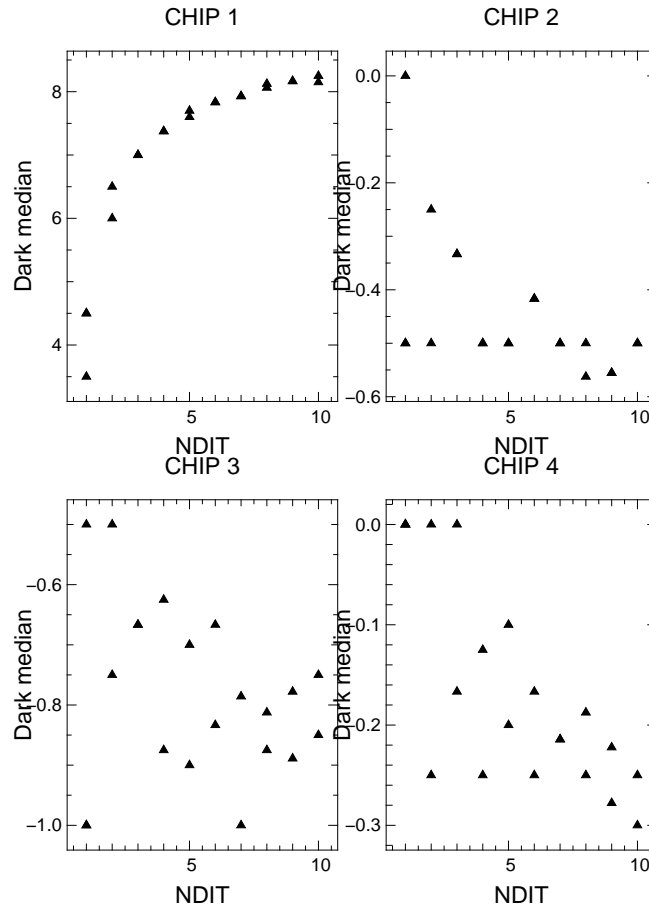


Figure 18: Trend of dark with NDIT in the 4 detectors.

### A.3 Detectors' relative sensitivity

We undertook a program to assess the relative sensitivities of the four HAWK-I chips, using observations of the high galactic latitude field around the  $z=2.7$  quasar B0002-422 at RA 00:04:45, Dec. -41:56:41 taken during technical time. The observations consist of four sets of  $11 \times 300$  sec AutoJitter sequences using the NB1060 filter. The four sequences are rotated by 90 degrees in order that a given position on the sky is observed by each of the four chips of the HAWK-I detector. The jitter sequences are reduced following the standard two-pass background subtraction workflow described in the HAWK-I pipeline manual. Objects have been detected with the SExtractor software (courtesy of Gabriel Brammer), including a  $0.9''$  gaussian convolution kernel roughly matched to the average seeing measured from the reduced images. Simple aperture photometry is measured within  $1.8''$  diameter apertures.

The resulting number counts as a function of aperture magnitude observed by each chip are shown in Fig. 20. As expected, the co-addition of the four jitter sequences reaches a factor of 2 (0.8 mag) deeper than do the individual sequences. The limiting magnitudes, here taken to be the magnitude where the number counts begin to decrease sharply and a proxy for the chip sensitivities, are remarkably similar between the four chips. We conclude that any sensitivity variations between the chips are within the 10%. While they do not appear to affect the overall

sensitivity, the image artefacts on CHIP2 caused by radioactivity events (see Fig. 19) do result in an elevated number of spurious detections (dashed lines in Fig. 20) at faint magnitudes, reaching 20% at the limiting magnitude for this chip. The number of spurious detections in the other chips is negligible (see Fig 20). This rate of spurious detections on CHIP2 should be considered as a conservative upper limit, as it could likely be decreased by more careful optimisation of the object detection parameters.

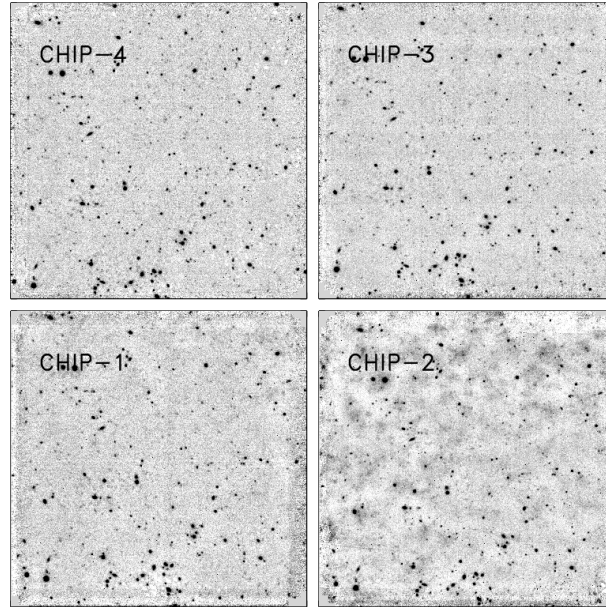


Figure 19: The field around the  $z=2.7$  quasar B0002-422 as seen in the 4 HAWK-I quadrants. Radioactivity effects are clearly visible in Q 2 (chip #78)

## B The HAWK-I filters

The 10 filters in HAWK-I are listed in Table 5. Please note that if you are interested in using the narrow band filters, you should contact the ESO Support Department before the proposal submission deadline (<https://support.eso.org>).

The filter curves as ascii tables can be retrieved from the [hawki instrument page](#).

**Note in particular that the Y band filter leaks and transmits 0.015% of the light between 2300 and 2500 nm.** All other filters have no leaks (at the  $<0.01\%$  level).

Table 5: HAWK-I filter summary.

| Filter name | central wavelength [nm] | cut-on (50%) [nm] | cut-off (50%) [nm] | width [nm] | transmission [%] | comments                      |
|-------------|-------------------------|-------------------|--------------------|------------|------------------|-------------------------------|
| Y           | 1021                    | 970               | 1071               | 101        | 92%              | LEAKS! 0.015% at 2300–2500 nm |
| J           | 1258                    | 1181              | 1335               | 154        | 88%              |                               |
| H           | 1620                    | 1476              | 1765               | 289        | 95%              |                               |
| $K_s$       | 2146                    | 1984              | 2308               | 324        | 82%              |                               |
| $CH_4$      | 1575                    | 1519              | 1631               | 112        | 90%              |                               |
| $Br\gamma$  | 2165                    | 2150              | 2181               | 30         | 77%              |                               |
| $H_2$       | 2124                    | 2109              | 2139               | 30         | 80%              |                               |
| NB1060      | 1061                    | 1057              | 1066               | 9          | 70%              |                               |
| NB1190      | 1186                    | 1180              | 1192               | 12         | 75%              |                               |
| NB2090      | 2095                    | 2085              | 2105               | 20         | 81%              |                               |

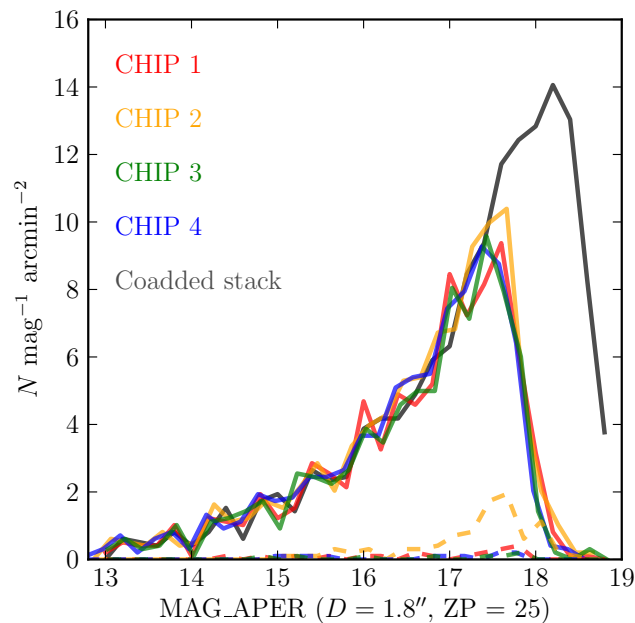


Figure 20: Number counts as a function of aperture magnitude for the four HAWK-I chips. The magnitudes as plotted adopt an arbitrary zero-point of 25 plus the relative zero-point offsets as monitored for the J filter (-0.14, +0.03, -0.23 mag for chips 2–4, relative to chip 1). The limiting magnitudes, i.e. the location of the turnover in the number counts, of the four chips are essentially identical within the measurement precision of this exercise ( $\leq 10\%$ ). Also shown are the number counts for a deep co-added stack of the four rotated and aligned jitter sequences. We use this deep image to assess the number of spurious sources detected on each chip: objects matched from the single chip image to the deeper image are considered to be real, while objects that only appear on the single-chip images are considered spurious. The number of spurious detections is negligible for chips 1, 3, and 4, though for chip 2 it reaches 20% around the limiting magnitude.

Optical ghosts (out of focus images showing the M2 and telescope’spiders) have been rarely found only with the NB1060 ( $\text{Ly}\alpha$  at  $z = 7.7$ ) & NB1190 ( $\text{Ly}\alpha$  at  $z = 8.7$ ) filters. As illustrated in Fig. 21, the ghost images are 153 pixels in diameter and offset from the central star in the same direction; however the latter varies with each quadrant and is not symmetric to the centre of the mosaic. The total integrated intensities of the ghosts are in both cases  $\sim 2\%$  but their surface brightnesses are a factor  $10^{-4}$  of the peak brightness in the stellar PSF.

The figure 22 summarizes the HAWK-I filters graphically.

## C The HAWK-I calibration plan

### C.1 Do you need special calibrations?

The calibration plan defines the default calibrations obtained and archived for you by your friendly Paranal Science Operations team.

**The calibration plan is what you can rely on without asking for any special calibrations.**

**However, these are indeed the only calibration that you can rely on without asking for special calibrations!!**

Thus, we strongly advise all the users to carefully think whether they will need additional calibrations and if so, to request them right in phase 1.

For example: is flat-fielding very critical for your program, i.e. should we acquire more flats (e.g. in your narrow band filters)? Would you like to achieve a photometry better than a few percent, i.e. do you need photometric standards



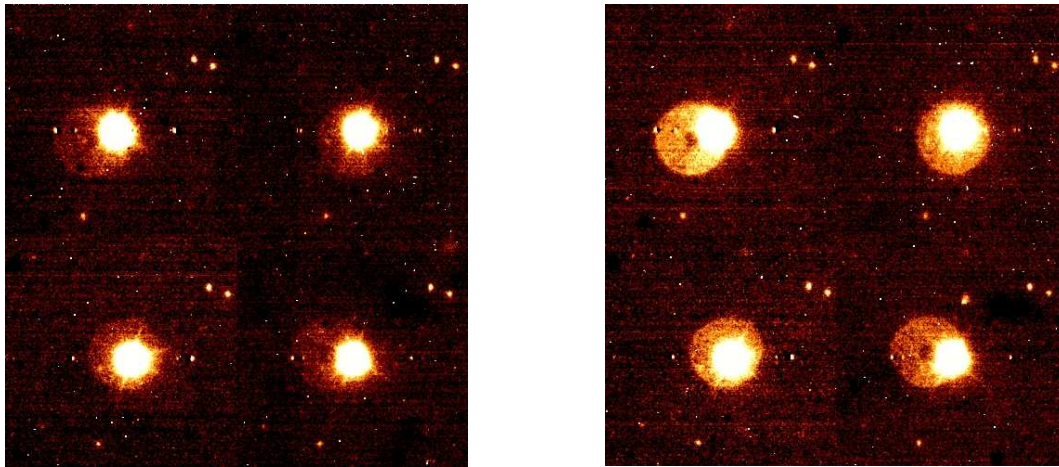


Figure 21: Smoothed enhanced images of the optical ghosts visible in the four quadrants for the NB1060 (left) & NB1190 (right) filters

observe right before/after your science frames? Is the homogeneity of the photometry critical for your program - i.e. should you ask for illumination frames close to your observations? Is the astrometry critical, i.e. should we acquire a full set of distortion and flexure maps around your run?

We would be more than happy to do all that for you *if you tell us so!* (i.e. if you mention it in phase 1 when submitting your proposal).

## C.2 The HAWK-I standard calibrations in a nutshell

Here is what we do, if we do not hear from you:

### HAWK-I – Calibration Plan

| Calibration              | number                      | frequency                | comments / purpose                           |
|--------------------------|-----------------------------|--------------------------|--|
| Darks                    | 10 exp. / DIT               | daily                    | for $\text{DIT} \times \text{NDIT} \leq 120$ |
| Darks                    | 5 exp. / DIT                | daily                    | for $\text{DIT} \times \text{NDIT} > 120$    |
| Twilight Flat-fields     | 1 set / filter              | within 21 days when used | broad-band filters (best effort basis)       |
|                          | 1 set / filter              | within 21 days when used | for narrow-band filters                      |
| Zero points              | 1 set / (broad-band) filter | daily                    | 2MASS Touchstone standard fields             |
| Colour terms             | 1 set                       | monthly                  | broad-band filters only (best effort basis)  |
| Extinction coefficients  | 1 set                       | monthly                  | broad-band filters only (best effort basis)  |
| Detector characteristics | 1 set                       | monthly                  | RON, dark current, linearity, ...            |

Note that the calibrations for Graal TTS-free mode do not require an LGS set-up. Hence, the above listed calibrations are performed in noAO mode and are also valid for the Graal TTS-free mode.

Please do not hesitate to contact us via <https://support.eso.org> if you have any questions!

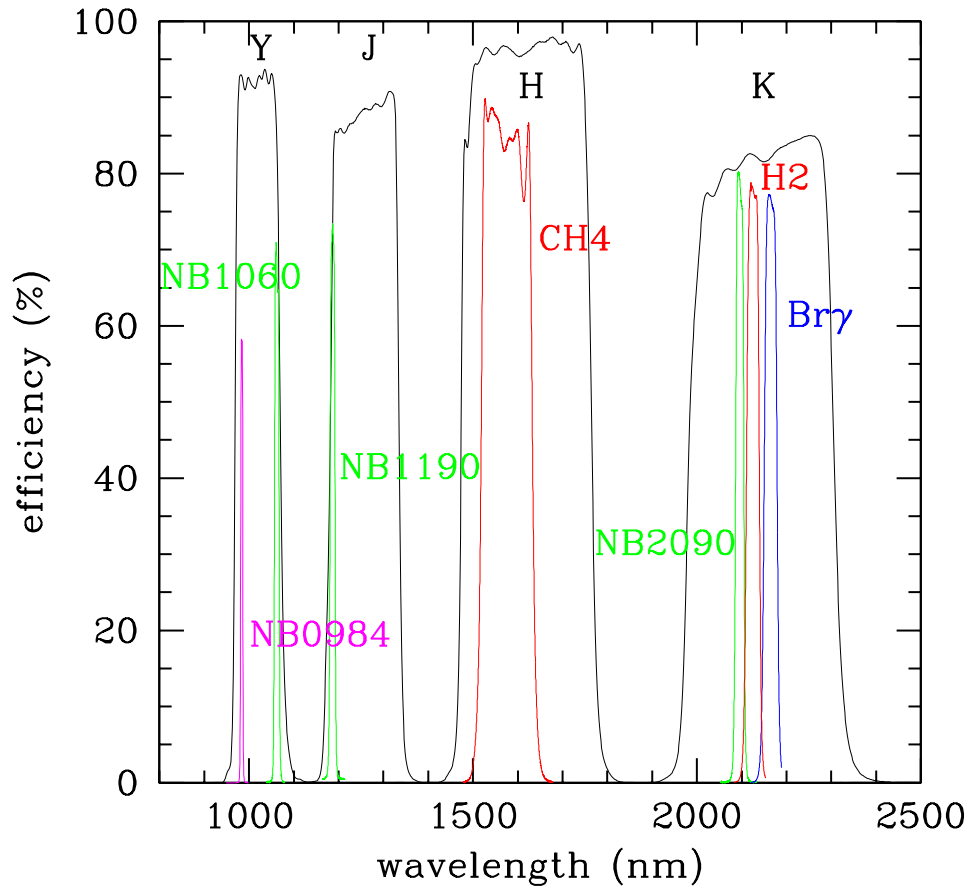


Figure 22: HAWK-I Filters. Black: broad-band filters Y, J, H, K<sub>s</sub>, Green: cosmological filters NB1060, NB1190, NB2090; Red: CH<sub>4</sub>, H<sub>2</sub>; Blue: Br $\gamma$ ; magenta: visitor filter NB0984 (now removed).

### C.3 Quality Control

All calibrations taken within the context of the calibration plan are pipeline-processed and quality- controlled by the Quality Control group at ESO Garching. Calibration and science raw data are available through the ESO User Portal. More information about the HAWK-I quality control can be found under <http://www.eso.org/observing/dfo/quality/HAWKI/qc/qc.html>. The time evolution of the most important instrument parameters like DARK current, detector characteristics, photometric zero-points and others can be followed via the continuously updated trending plots available on the HAWK-I QC webpages ([http://www.eso.org/observing/dfo/quality/index\\$\\_\\$hawki.html](http://www.eso.org/observing/dfo/quality/index$_$hawki.html)).



## D HAWK-I Fast Jitter Mode

### D.1 Description

This section describes a mode for high-cadence and high time-resolution observations with HAWK-I: the fraction of time spent integrating is typically  $\sim 80\%$  of the execution time, and the minimum DIT (MINDIT) is in the range  $\sim 0.01$ - $0.1$  sec. The mode is useful in two observing scenarios: (i) studies of quickly varying sources that require good sampling of the light curves (i.e., X-ray sources); (ii) studies of events with limited duration that can't be re-observed, so dead times are undesirable (i.e., transit timing variations of extrasolar planets). A good example of a combination of the two are Lunar occultations (Richichi et al. 2013, AJ, 146, 59).

This is achieved by two measures:

**First**, by windowing down the detectors to speed up the observations (in other words, to shorten the MINDIT) and to decrease the overheads for data transfer. For example, the MINDIT for a  $64 \times 64$  px ( $\sim 6 \times 6$  arcsec) window, which is about a reasonable minimum for observing, is 0.1022 sec. Historically, the MINDIT was lower, but increased noise in the detectors led to slowing down the readout speed, and this increased it to the present value. Unfortunately, this effectively makes it impossible to carry out observational programs that require milli-seconds scale resolution.

Archival users should be aware that initially (from 2010 to mid-2012) the mode suffered from extra overheads of 0.15 sec plus one MINDIT (the exact value depends on the detector windowing but for the most likely window sizes it is a few tens of a second or larger; an upper limit for a non-windowed detectors is  $\text{MINDIT} \sim 1.8$  sec) associated with each DIT. This made observations with very high cadence requirements problematic but as of mid-2012 the new faster *ReadRstRead* detector readout mode, – described below, – was implemented.

Note that the windows are not located at the center of the HAWKI field of view, i.e. if the telescope is preset to the target coordinates, the target will fall into the central gap between the four detectors. Therefore, one must calculate an offset, placing the target onto one of the detectors, preferably close to where the detector windows are.

**Second**, the new detector readout mode *ReadRstRead* is used. It is similar to the *Double Correlated* where the sequence is:

cycle 1:

read the detector,  
reset the detector,  
read the detector,  
integrate for a time = DIT, sec

cycle 2:

read the detector,  
reset the detector,  
read the detector,  
integrate for a time = DIT, sec

etc..

The frame is reconstructed by subtracting the second read of the first cycle from the first read of the second cycle, and so forth.

The difference between the *Double correlated* and *ReadRstRead* modes is that when one pixel is reset or read, the rest of the pixels integrates; in case of the "normal" *Double Correlated* readout mode the pixel waits until all other pixels are reset/read which implies a read time of MINDIT for every DIT. *ReadRstRead* is therefore faster, since this waiting phase is absent and the overheads are of the order of a few microseconds per DIT—the time needed to reset/read only one individual pixel. This mode has only one single destructive readout, so DET.SATLEVEL is not possible in this mode.

The integrations of individual pixels in *ReadRstRead* mode are offset with respect to each other, so the integration of the last to be reset/read pixel starts MINDIT seconds after the integration of the first pixel to be reset/read. Usually, it is safe to ignore this effect—either because the  $\text{DIT} \gg \text{MINDIT}$  (as is usually the case for exoplanet observations) or because the window is almost as small as the target size, so the signal from the target is averaged over nearly all pixels from the window (as is the case of the Lunar occultations).

The Fast Jitter mode is intended for observations of extremely bright objects that require short DITs to avoid saturation, and small overheads, to increase the efficiency, i.e. exo-planet transits.

**Update:** The fast photometry may be familiar to the users of fast jitter of ISAAC, NaCo, VISIR, and SofI. The

main advantage of HAWK-I in comparison with these instruments is the wide field of view that allows a better selection of bright reference sources for relative photometry, and the favorable pixel scale.

## D.2 Implementation

The Fast Photometry templates are discussed in details further, but for clarity we will point out here that they work in a markedly different way, with respect to the templates for other ESO instruments: **the windowing parameters are present only in the acquisition template, and their values are carried over to the science template(s) by the Observing Software (OS)** using designated common memory area. So, one can not skip the acquisition if it is necessary to modify the windowing parameters. If the acquisition is skipped, the science template will use the values from the last acquisition execution. If an OB has been aborted, the windowing parameters are remembered by the observing software (as long as the Detector Control System (DCS) and OS panels have not been reset/restarted), so the OB can simply be restarted, skipping the acquisition.

Occasionally, during the execution of an OB a new acquisition image is not loaded automatically in the real-time display (RTD). In this case, one can re-load the last acquisition image in that RTD and re-draw the location of the windows by clicking on “set-up and draw” from the pop-up that BOB opens with the acquisition template.

**Important:** a measure to reduce the load on the IRACE controller is to click on *stop* displaying the images on the RTD during the observations. This is achieved by pressing the Stop button on the RTD panel.

**NOTA BENE:** The IRACE is set to default at the end, and this is critical for the observations afterwards. If an OB is aborted for some reason before this step, the IRACE remains in hardware windowing mode, with the window size defined during the OB, and with the *store-in-data- cube* mode ON.

### D.2.1 Detector Windowing

For speeding up the observations the HAWK-I detectors are windowed at hardware level, so only the pixels that fall within the user-defined windows are actually read. In contrast, in case of software windowing the entire detectors are read, and only the pixel values within the user-defined windows are stored, so there is no gain in speed. The hardware windowing is hard-coded in the templates, and does not require any further action from the user.

Each HAWK-I detector is read in 16 vertical stripes. The stripes span  $128 \times 2048$  px, and each of the detectors spans  $2048 \times 2048$  px. **One window is defined in each stripe, but the locations of the windows are not independent**, i.e. they all move together in a consistent manner that will be described further below.

Therefore, the total number of windows for each HAWK-I frame is  $4 \times 16 = 64$  because HAWK-I is made of 4 detector arrays. Along the X-axis the windows can be contiguous or separated *within* each detector; even contiguous windows within the detector offer only sparse coverage on the sky because the four detectors themselves only offer a sparse coverage of the focal plane, i.e. there is space between the arrays (gaps), so one can not have a single contiguous window across the entire focal plane. The situation closest to that are four contiguous windows—one across each of the four detectors. An additional constraint is that the windows must be centered within the stripes. Since the stripes are 128 pixels wide – an even number, – the width of the windows (defined by DET.WIN.STARTX, see below) must also be an even number.

The detector windows are described by the following parameters:

- DET.WIN.STARTX and DET.WIN.STARTY define the starting point of the window **within an individual stripe**. The X-axis on all detectors increases in the same direction, but the Y-axis on the upper and the lower detectors increases in opposite directions, so when the values of DET.WIN.STARTX and DET.WIN.STARTY increase, the starting points of the windows move to the right along the X-axis, and towards the central gap along the Y-axis. Note that these parameters are different at the software level from the parameters DET.WIN.STARTX and DET.WIN.STARTY used to define the windowing in other HAWK-I observing modes!!

Values larger than 100 px are recommended for DET.WIN.STARTY because the background at the edges of the detectors is higher due to an amplifier glow. The allowed value ranges for DET.WIN.STARTX and DET.WIN.STARTY are 1...128 and 1...2048, respectively, but if they are set to 128 and 2048, the window will only be  $1 \times 1$  px, so the users should select smaller starting values to leave room for an ample size of the windows.

- DET.WIN.NX and DET.WIN.NY define the sizes in pixels of the windows in each individual stripe. For example, if the user wants to define a window of  $18 \times 28$  px on each stripe, the corresponding values

of DET.WIN.NX and DET.WIN.NY will be 18 and 28, respectively. These values will produce a fits file that contains a 3-dimensional data cube with  $576 \times 56 \times \text{NDIT}$  because of the 16 stripes in each of the two detectors along the X-axis ( $18 \times 16 \times 2 = 576$ ) and the two detectors along the Y-axis ( $28 \times 2 = 56$ ). The allowed values are 1...128 and 1...2048 for DET.WIN.NX and DET.WIN.NY, respectively. However, **the users should take care that the starting point plus the size of the window along each axis do not exceed the size of the stripe along that axis: 128 or 2048, respectively for X and Y.**

Figure 23 shows examples of various detector window definitions. For instance, an increase of the parameter DET.WIN.STARTX would move the violet set of windows towards the yellow set, if the other parameters are kept fixed. Similarly, an increase of the parameter DET.WIN.STARTY would move the violet set towards the solid black set. The dashed black line set corresponds to DET.WIN.NX=128 ( $128 \times 16$  stripes  $\times 2$  detectors = 4096 px in total along the X direction) that defines contiguous windows (see below).

An interesting special case is to define contiguous regions (i.e. the windows on the individual stripes are as wide as the stripes themselves, so there are no gaps along the X-axis) - one has to use for example: DET.WIN.STARTX=1, DET.WIN.STARTY=48, DET.WIN.NX=128 and DET.WIN.NY=32, corresponding to windows on the stripes with sizes of  $128 \times 32$  px ( $\sim 13.3 \times 3.3$  arc-secs), gives MINDIT=20 milli-secs. Note that the stripes are 128 px wide, so this is indeed a contiguous region on each of the detectors, with size  $2048 \times 32$  px ( $\sim 217.7 \times 3.4$  arcsec).

Typically, the choice of window sizes is the result of a compromise between a few conflicting requirements:

- faster photometry (i.e., smaller overheads, smaller MINDIT, higher time resolution), requires **smaller** window sizes;
- more accurate photometry (i.e., brighter and more reference stars, wider clear area to measure the sky level, wider margin for human errors during the acquisition, leeway for target drift across the window because of poor auto-guiding or atmospheric refraction since the target is observed in the NIR, and the guiding is in the optical) requires **wider** window sizes;
- smaller data volume requires smaller windows;
- higher data cadence (i.e., less gaps between files for transfer, fits header merging) requires smaller window.

**To simplify and standardize the observations, and to minimize the day-time calibration time, the following constraints on the window parameters are imposed:**

- Only contiguous windows that span entirely the width of the detectors are offered, so DET.WIN.NX must always be set to 128 ( $\sim 13.3$  arcsec), and DET.WIN.STARTX - to 1. Therefore, the total size of the output file along the X axis is always  $128 \times 32 = 4096$  pixels.
- Only three values for the window height are allowed, so DET.WIN.NY can be set to 32, 64 or 128 pixels ( $\sim 3.3$ , 6.7 or 13.3 arc-seca, respectively). There is no restriction on where the windows are located, so the users are free to set DET.WIN.STARTY to any possible value (from 1 to  $2048 - \text{DET.WIN.NY}$ ).

If the scientific goals of the program require different window sizes, the users must contact the User Support Department via <https://support.eso.org>. to check if they are technically feasible/acceptable, and if this is the case - to ask for a waiver.

## D.2.2 Data Products and Cube Sizes

The data product is a fits file containing cubes with slices made from the tiled-together images of all windows (windows in each stripe), i.e. spliced together without the gaps that will be present between the individual windows (such gap occur always because of the gaps between the detectors; extra gaps occur if DET.WIN.NX is smaller than 128 and if DET.WIN.NY is smaller than 2048). The FastJitt generates as many files (each containing a cube) as the number of the jitters in the OB.

The cubes contain one extra slice (i.e. NDIT+1 instead of NDIT) because the last slice is the average of all NDITs. In Fast Jitter mode, the sliced in the generated cubes are:

*1st DIT (a difference between the 2 reads, separated by DIT seconds)*

*2nd DIT (a difference between the 2 reads, separated by DIT seconds)*

...

*INT (an averaged frame of all previous slices)*

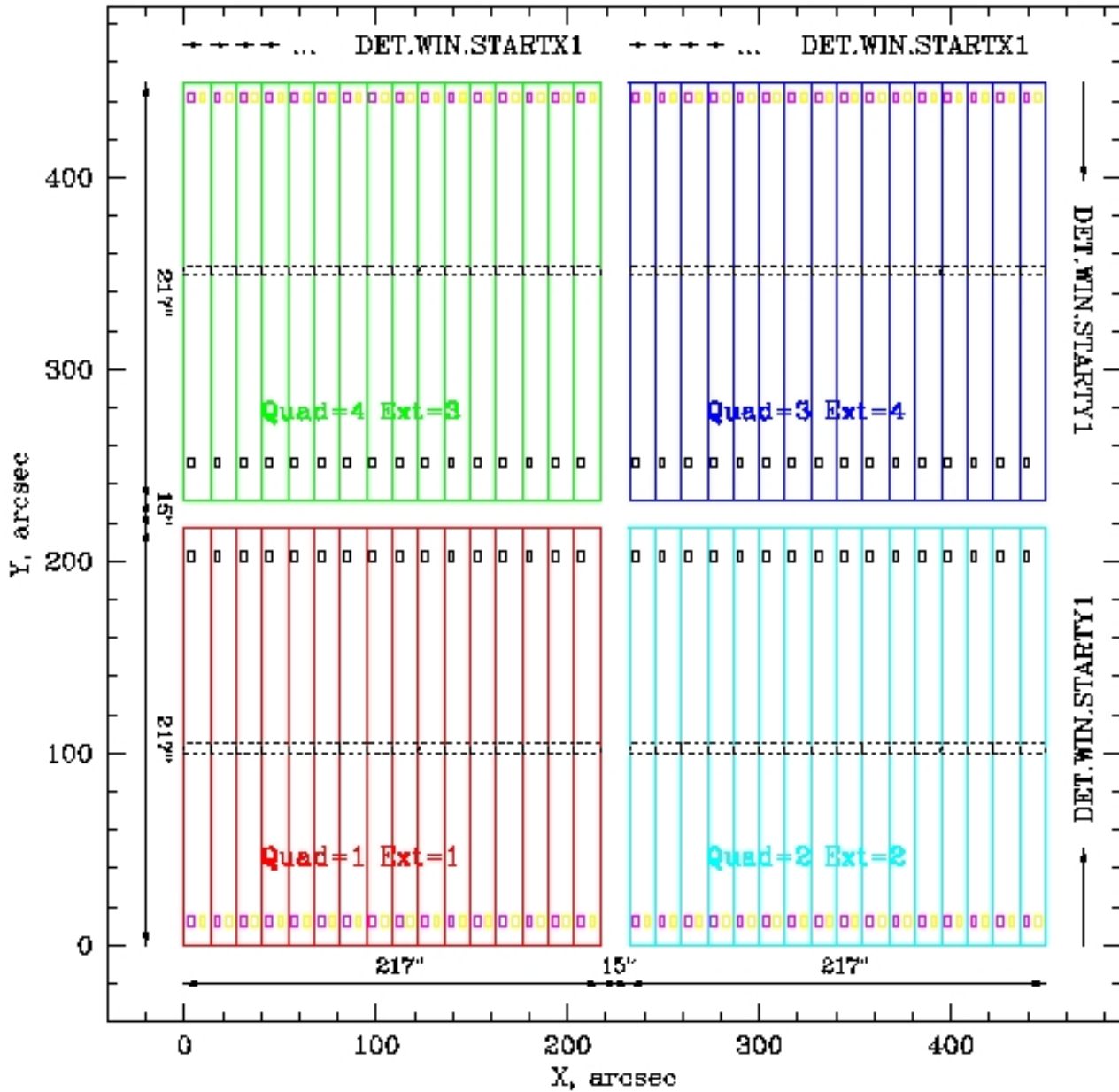


Figure 23: Definition of the windows. The location of the four HAWK-I detectors on the focal plane is shown, as well as the 16 stripes in which each detector is being read. The sizes of the detectors and the gaps, projected on the sky in arc-secs are also given. The binaries generated from quadrants 1, 2, 3, and 4 are usually (but not always) stored in fits extensions 1, 2, 4, and 3. Arrows indicate the direction in which the parameters DET.WIN.STARTX, DET.WIN.STARTY, DET.WIN.NX and DET.WIN.NY increase. Note, that the parameter DET.WIN.STARTX defines the starting point of the window, counted from the beginning of each detector stripe, not from the beginning of the detector. All these parameters are defined in pixels, although this figure is plotted in arc-secs. As examples, four different sets of windows are shown in violet, yellow, solid and dashed black lines.

Therefore, if no frames are lost, the generated cube contains:

$$NAXIS3 = NDIT + 1 \quad (1)$$

slices.

Frame loss, that plagues some other “fast” instruments, has not been noticed during the typical applications of the HAWK-I fast photometry modes. Most likely, because of the slowing down of the detector read speed, that increased the minimum DITs. This problem usually occurs when the product of NX and NY is relatively large, and DIT is close to MINDIT, so the IRACE has to transfer large data volume quickly. To check for frame losses, verify that NAXIS3 header keyword is equal to estimates, given above.

The HAWK-I fast mode is subject to a maximum cube limitation, similarly to ISAAC and Sofl. The buffer size in this case is 512 Mb. If the cube size exceeds the 512 Mb limit, the observations will be split into multiple file extensions, but the headers of all extensions will contain the DATA-OBS information for the start of the observation, not for the start of the given extension. Each extension will also have its own smaller header. This poses a problem if the aim of the program is to achieve high timing accuracy because the data transfer time and the fits header merging time are subject to variations depending on the load on the local network and on the instrument workstation. These variations are hard to quantify, so we recommend to keep the cube size below 512 Mb. In addition, the overheads are larger if the cube is split into individual files, because they have to be merged, so an extra time to copy the entire cube into a single file is necessary. Finally, the OS supports a maximum size of 2 Gb, and if the combined size exceeds that, the merging fails, and the OB is aborted.

Therefore, the NDIT must be limited to keep the file size below 512 Mb.

The user has two options to adjust the cube size:

- to change the window size defined by DET.WIN.NX , or
- to change the number of slices in the cube defined by NDIT.

Often the former is not possible, because the size is set by other considerations, i.e. the angular separation on the sky between a target and a reference source, the required low MINDIT or the need to have large enough window to avoid slit-like losses (especially in case of poor seeing). Therefore, reducing the NDIT may be the only solution to this problem.

The cube size for FastJitt mode (that stores restored images) is:

$$(NX * 32) * (NY * 2) * NDIT * 4 \geq (512 \times 1024 \times 1024) = 536870912 \quad (2)$$

The maximum acceptable NDIT is:

$$NDIT_{max} \leq (536870912 / ((NX * 32) * (NY * 2) * 4)) - 1 \quad (3)$$

The “-1” leaves space for the averaged image, that is always stored in the last slice of the cube.

### D.2.3 Minimum DIT, Overheads, and Frame Losses

The MINDIT depends strongly on the size and weakly on the location of detector windows.

The MINDITs and the execution times for some of the offered windowing parameter combinations are listed in Table 6.

The table shows that the overheads depend mainly on the window size (because of the amount of pixels that need to be read and transferred) while the location of the window has minor effects. The “faster” windows are located close to the outer edges of the detectors, i.e. with smaller values of STARTY. However, it is recommended to avoid setting STARTY=1 px, because the edges of the detectors usually suffer from stronger cosmetic defects. The experience shows that these effects are smaller starting from STARTY=100-150 px.

The time spent on the acquisition is a matter of how many fine adjustments are needed. The absolute minimum of the acquisition, without any telescope movement, or movement of instrument wheel, is ~100 sec. This is important to remember in case of aborting and restarting the OB with acquisition. Therefore, if the OB has to be aborted for some reason, and there is no need to make adjustments, it is better to skip the acquisition template.

Table 6 also shows the execution times for a few extreme or typical cases: if the DIT is set to the smallest available value for a given windowing configurations, and if the DIT is set to 0.1-0.2 secs, which are often requested by the users.

Table 6: Timing Parameters. The execution times were rounded to 1 sec. The overheads are given for executing  $NEXP = 5$  exposures, in stare mode (i.e., with jitter box size  $JITTER.WIDTH = 0$  and  $NOFFSET = 1$ ). The 32 and 2 multiplication factors are given to remind the user that the NX and NY parameters are the total width of the detector windows across the entire set of stripes. The readout mode is ReadRstRead. STX and STY stand for STARTX and STARTY, respectively. (\*): this is a non standard case!

| STX<br>px | NX<br>px       | STY<br>px | NY<br>px  | MINDIT<br>sec | Max.<br>NDIT | DIT<br>sec | NDIT | Integr.<br>Time<br>sec | Exec.Times<br>1 exp. NEXP=5<br>sec | Frame<br>loss<br>% |      |
|-----------|----------------|-----------|-----------|---------------|--------------|------------|------|------------------------|------------------------------------|--------------------|------|
| 1         | 32×32=1024 (*) | 1         | 32×2= 64  | 0.051096      | 511          | 0.051096   | 511  | 26.110056              | 28                                 | 160                | 1.2  |
| 1         | 128×32=4096    | 1         | 32×2= 64  | 0.051864      | 511          | 0.051864   | 511  | 26.502504              | 28                                 | 165                | 7.2  |
| 1         | 128×32=4096    | 1         | 32×2= 64  | 0.051864      | 511          | 0.1        | 511  | 51.1                   | 53                                 | 286                | 1.3  |
| 1         | 128×32=4096    | 1         | 32×2= 64  | 0.051864      | 511          | 0.2        | 511  | 102.2                  | 104                                | 542                | 2.4  |
| 1         | 128×32=4096    | 1         | 32×2= 64  | 0.051864      | 511          | 0.2        | 128  | 25.6                   | 28                                 | 159                | 1.0  |
| 1         | 128×32=4096    | 1         | 64×2=128  | 0.1037        | 255          | 0.1037     | 255  | 26.4435                | 28                                 | 164                | 4.6  |
| 1         | 128×32=4096    | 1         | 128×2=256 | 0.2074        | 127          | 0.2074     | 127  | 26.3398                | 28                                 | 166                | 11.2 |
| 1         | 128×32=4096    | 1024      | 32×2= 64  | 0.066186      | 511          | 0.066186   | 511  | 33.821046              | 35                                 | 199                | 3.4  |
| 1         | 128×32=4096    | 1024      | 64×2=128  | 0.1180        | 255          | 0.1180     | 255  | 30.0900                | 32                                 | 181                | 4.4  |
| 1         | 128×32=4096    | 1024      | 128×2=256 | 0.2217        | 127          | 0.2217     | 127  | 28.1559                | 30                                 | 176                | 7.6  |
| 1         | 128×32=4096    | 2016      | 32×2= 64  | 0.080074      | 511          | 0.080074   | 511  | 40.917814              | 43                                 | 236                | 2.6  |
| 1         | 128×32=4096    | 1984      | 64×2=128  | 0.1315        | 255          | 0.1315     | 255  | 33.5325                | 36                                 | 200                | 3.4  |
| 1         | 128×32=4096    | 1920      | 128×2=256 | 0.2342        | 127          | 0.2342     | 127  | 29.7434                | 32                                 | 182                | 2.0  |

For convenience, we list the integration time for a single data cube (equal to  $NDIT \times DIT$ ), the execution time for a single cube, and the execution time for a template that generates five cubes ( $NEXP=5$ ). The test were carried out with  $NJITT=1$ ,  $JITTER.BOX=0$ , the *Read-speed factor* was 8, and the *Read-speed add* was 0. The last two parameters are low-level detector controller parameters, they are controlled by the observing templates, and they are fixed at these values for technical reasons beyond the scope of this document; we list them here just for completeness. The filter for the observations was set up in the acquisition template; if it must be changed in the science template, there will be additional overheads related to the filter movement.

The overhead per template is typically  $\sim 30$ – $33$  sec. Let's consider the last case in the table: five exposures of  $NDIT \times DIT = 29.7434$  sec collect together 148.717 sec of integration, leaving 33 sec in overheads, up to the template execution time of 182 sec. These  $\sim 33$  sec are build up as follows:  $\sim 2$  sec to process the template and to send a set up command to the instrument – this could be much longer if there is a filter change;  $\sim 10$  sec to set up the IRACE detector controller,  $\sim 2$ – $3$  sec to transfer every data cube and to merge the fits file and its header,  $\sim 10$  sec to set up the IRACE detector controller back to the “standard” set up at the end of the template. A detailed time line of the execution is shown in Table 7. The overheads listed above may vary by 1–2 sec.

Finally, the HAWKI Fast Photometry mode suffers from frame loss, especially if the DIT is close to the the MINDIT for the given windowing configuration. Table 6 lists the frame loss rate in percentages. The frame losses increase with the size of the window, and for a given window size they decrease with increasing DIT, as can be seen from the few examples for  $NX=128$ ,  $NY=32$ . Last but not least, the frame losses depend on the network load: the experience shows that just turning off the RTD during the observations can reduce the frame loss by 2–3%. Unfortunately, other loads on the network can not be controlled by the operators, which can easily leads to uncertainty in the frame loss rate of 2–3%, as our experiments has shown. Frame losses for the window sizes listed in the Table 6 practically disappear for  $DIT=0.5$ – $1.0$  sec.

Table 7: Example Timing Parameters of the last case considered in Table 6.

| Action           | Time     |
|------------------|----------|
| start template   | 21:04:38 |
| IRACE set up     | 21:04:40 |
| start exposure 1 | 21:04:50 |
| end exposure 1   | 21:05:22 |
| start exposure 2 | 21:05:22 |
| end exposure 2   | 21:05:54 |
| start exposure 3 | 21:05:54 |
| end exposure 3   | 21:06:26 |
| start exposure 4 | 21:06:26 |
| end exposure 4   | 21:06:58 |
| start exposure 5 | 21:06:58 |
| end exposure 5   | 21:07:30 |
| IRACE set up     | 21:07:40 |
| end template     | 21:07:40 |

## D.3 Preparation and Observation

### D.3.1 OB Naming Convention

Following the common convention for the fast modes:

*FastJitter* OBs should start with the prefix "FAST" in their name,

### D.3.2 OB Requirements and Finding Charts

The finding chart requirements are the same as for the other VLT instruments.

The typical accuracy of the VLT pointings is below 1 arcsec. **However, the simple preset *HAWKI\_img\_acq\_Preset* can not define the correct detector windowing for the fast mode! The windowing is defined only in the specialized acquisition template it *HAWKI\_img\_acq\_FastPhot*. Therefore, *HAWKI\_img\_acq\_FastPhot* must be executed at least once, and the windowing parameters should be kept the same during the entire sequence.**

Sec. [D.4](#).

### D.3.3 Observing Modes

The FastJitter mode is now offered both in Service and Visitor mode.

### D.3.4 Calibration Plan

- Darks taken with the same windowing and readout mode,
- Twilight Flats, non-windowed and with the same filters as the science observations are offered, the users only have to excise from them the necessary windows; we compared windowed and non-windowed  $K_S$  flats, and found no significant difference (Fig. [24](#)).

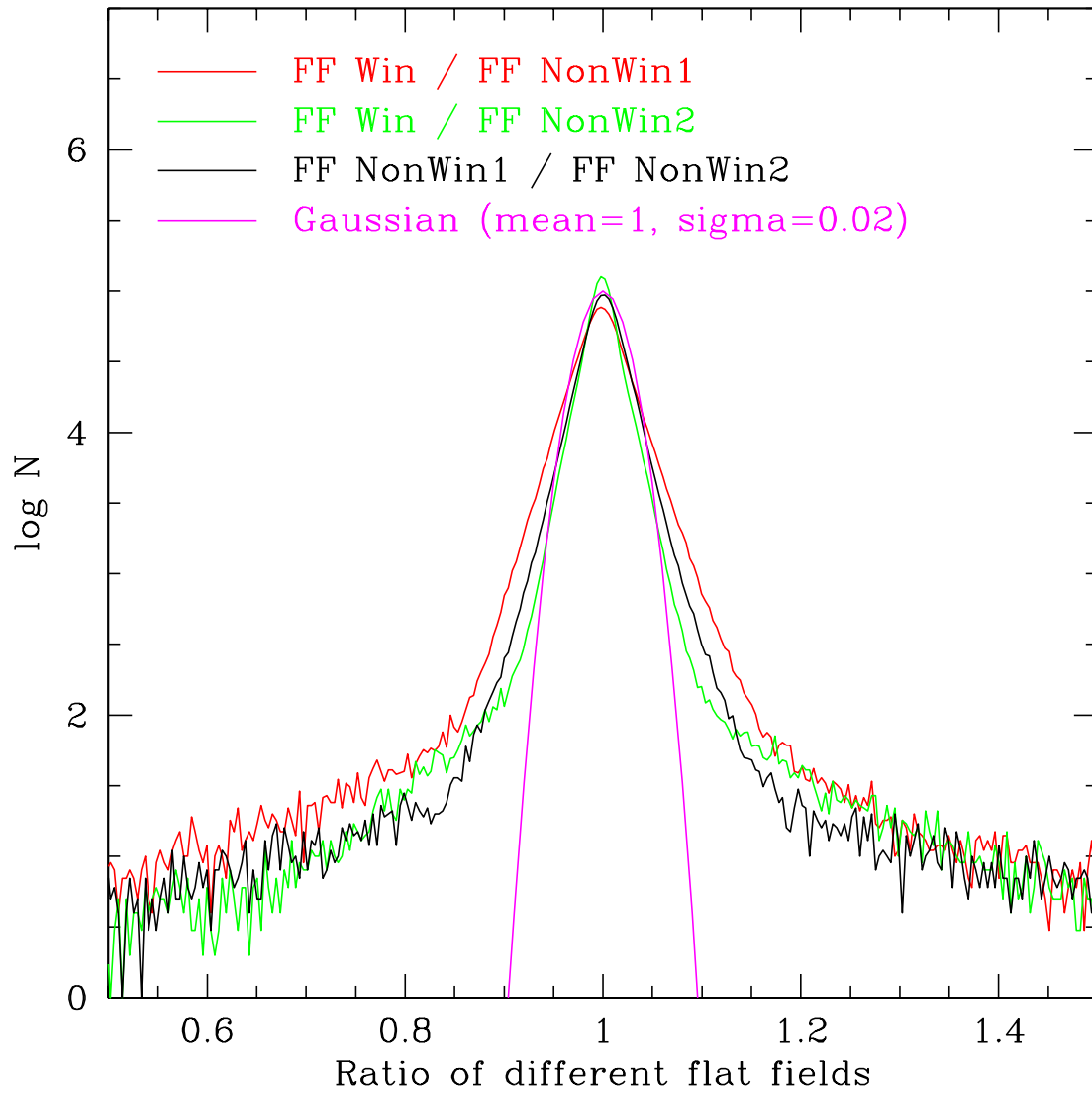


Figure 24: Histograms of the ratios between a windowed and two non-windowed  $K_S$  twilight flats. For comparison, the ratio of the two non-windowed flats and a Gaussian function is also shown.



### D.3.5 FITS Files Names

The file names for the fast mode contain “FAST” for clarity. The extensions SAMPLE and DIT are also appended to the FITS file name.

## D.4 Template Guide

### D.4.1 Acquisition: *HAWKI\_img\_acq\_FastPhot* and *HAWKI\_img\_acq\_LGS\_FastPhot*

The detector windowing parameters (DET.WIN.STARTX, DET.WIN.STARTY, DET.WIN.NX and DET.WIN.NY) are defined in this template. They are used to draw on the RTD the locations of the 32 windows. These parameters are stored in OS registers, and used by the science template later. They can be accessed by the science template even if it has been aborted and restarted multiple times, as long as the OS has not been stopped and restarted.

The action sequence performed by the template includes:

1. Preset the telescope, set up the instrument (no windowing at this stage, the full field of view is shown on the RTD).
2. Move to the sky position, take a non-windowed image, ask the operator to save it in the RTD and to turn on the sky subtraction
3. Take a non-windowed image of the field of view, ask the operator if an adjustment is necessary. Note that the adjustment here includes both the telescope pointing (and field of view orientation), and the detector windowing parameters. At this stage the operator is expected to press the “draw” button that draws on the RTD the windowing as defined in the acquisition template. The operator can modify it at any time from now on (by typing numbers on the pop up window), but has to redraw to have the latest version shown on the RTD.
4. If the operator gives a negative answer, the template acquires an image, saves it, and then ends. Otherwise, an offset window is opened on the RTD to let the operator to define an offset and rotator angle offset (and to modify the windowing parameters).
5. The offsets (including the rotator offset) are sent to the telescope and after they are executed, the template returns to item 3 where it takes another non-windowed image and so on.

### D.4.2 Science template: *HAWKI\_img\_obs\_FastPhot*

This template is similar to the *ISAACLW\_img\_obs\_FastPhot* except that it takes the detector windowing parameters from the OS registers, so these parameters can't be modified from within *HAWKI\_img\_obs\_FastPhot*.

The template operates in one mode : *FastJitter*. In *FastJitter* mode, the telescope can jitter in the sky and many data cubes (one per offset) can be produced within one template.

Action sequence performed by the template is identical to that of the *HAWKI\_img\_obs\_AutoJitter* template:

1. Sets up the instrument, including selection hardware detector windowing.
2. Performs a random offset (most users are likely to set the jitter box size to zero to keep the objects located on the same pixels, which should reduce systematic effects from imperfect flat fielding).
3. Acquires images stored in a cube, and continues as long as the number of the frames in the cube is equal to the value of the parameter DET.NDIT (this parameter defines the length of the cube). The number of cubes acquired at each offset position is defined by SEQ.NUMEXP.
4. Goes back to step and repeats the actions until SEQ.NUMOFFSET offsets are executed.

Specific details:

- The new windowing parameters (DET.WIN.STARTX, DET.WIN.STARTY, DET.WIN.NX and DET.WIN.NY) are not accessible to the user from this template.
- Readout mode is set to *DoubleRdRstRd* because for now this is the only one for which the new windowing is implemented.

- The hardware windowing is set to *True* (implicitly for the user).
- The store-in-cube option is set to *True*.

### D.4.3 Calibration templates: *HAWKI\_img\_cal\_DarksFastPhot*

Twilight flats for this mode are obtained with the normal non-windowing *HAWKI\_img\_cal\_TwFlats* template making the dark current calibration template *HAWKI\_img\_cal\_DarksFastPhot* the only unique calibration template for the fast mode. It is similar to the usual dark current template *HAWKI\_img\_cal\_Darks*, with the execution of the hardware windowing and the storage of the data in cubes. The parameters for filter, DIT, and NDIT are lists, allowing to obtain multiple darks in one go.

Specific details:

- The new windowing parameters (DET.WIN.STARTX, DET.WIN.STARTY, DET.WIN.NX and DET.WIN.NY) define the detector windowing. As in the science template, they are used to window the detectors but unlike the science template they are explicitly definable and accessible by the users.
- The previous parameters are not available in the calibration templates. All the calibration are taken as reconstructed images.
- Readout mode is set in the template implicitly to *Double RdRstRd* because for now this is the only one for which the new windowing is implemented.
- The hardware windowing is set to *True*.
- The store-in-cube option is set to *True*.